Analysis of Short-term Microbial Eukaryotic Community Dynamics in the Greifswalder Bodden

Analyse der kurzzeitigen Dynamik mikrobieller eukaryotischer Gemeinschaften im Greifswalder Bodden

Master Thesis in Marine Biology

Laura Menke

Submitted on: 30.03.2026

University of Rostock

&

Leibniz Institute for Baltic Sea Research, Warnemünde (IOW)

https://doi.org/10.18453/rosdok_id00005641

Primary supervisor:

Dr. Ingrid Sassenhagen

IOW

Department of Biological Oceanography

Phytoplankton Ecology

ingrid.sassenhagen@io-warnemuende.de

Secondary supervisor:

Dr. Christiane Hassenrück

IOW

Department of Biological Oceanography

Bioinformatics and Biomics data

christiane.hassenrueck@io-warnemuende.de

Table of Contents

List of Figures

List of Figures (Appendix)

List of Tables

List of Tables (Appendix)

Summary

Microbial eukaryotic protists represent a significant proportion of global biodiversity and play crucial roles in aquatic ecosystems. The composition of protist communities is dynamic and dependent on abiotic and biotic factors. While microscopy has traditionally been used to identify protists, its efficiency is often limited. With the help of eDNA metabarcoding, it is possible to identify large quantities of organisms in a short time. The aim of this study was to investigate the community of microbial eukaryotes in the Greifswalder Bodden in July 2025 using 18S rRNA metabarcoding, focusing on short-term dynamics and the potential influence of environmental parameters.

Size fractionation provided deep insights into the protist community and revealed distinct communities. The two size fractions ≥5 (large) and 0.22–5 (small) µm differed significantly in their alpha and beta diversity, as well as in their overall taxonomic composition.

Furthermore, short-term temporal changes varied in the two communities. The alpha indices Shannon and Inverse Simpson showed trends indicating that the small fraction shifted from a community dominated by a few taxa to a more even distribution over time. Conversely, the large fraction became less even toward the end of the month as individual taxa increased in their relative abundance. Temporal turnover analysis confirmed these shifts, with Jaccard values (0.56 to 0.62) reflecting a moderate exchange of taxa in both fractions throughout July.

The analysis of environmental drivers showed that nitrite correlated significantly with the large fraction, while dissolved oxygen and nitrite were associated with the small fraction. In summary, these results highlight the dynamic nature of the protist community in the Greifswalder Bodden and demonstrate that short-term changes as well as correlations with environmental parameters can differ in a size-specific manner.

Zusammenfassung

Mikrobielle, eukaryotische Protisten repräsentieren einen großen Teil der globalen Biodiversität und spielen in aquatischen Ökosystemen wichtige Rollen. Die Zusammensetzung der Protistengemeinschaften ist dynamisch und von abiotischen und biotischen Faktoren abhängig. Während traditionell die Mikroskopie genutzt wurde, um Protisten zu bestimmen, ist deren Effizienz oft begrenzt. Mithilfe von eDNA-Metabarcoding ist es hingegen möglich, große Mengen von Organismen in kurzer Zeit zu identifizieren. Das Ziel dieser Studie war es, die Gemeinschaft mikrobieller Eukaryoten im Greifswalder Bodden im Juli 2025 mittels 18S rRNA-Metabarcoding zu untersuchen, wobei der Fokus auf kurzzeitige Dynamiken und dem potenziellen Einfluss von Umweltparametern lag.

Die Größenfraktionierung ermöglichte einen tieferen Einblick in die Protistengemeinschaft und machte deutliche Unterschiede zwischen den Fraktionen sichtbar. Die beiden Größenfraktionen ≥5 (groß) und 0.22–5 (klein) µm unterschieden sich signifikant in ihrer Alpha- und Beta-Diversität sowie in ihrer taxonomischen Zusammensetzung.

Darüber hinaus variierten die kurzzeitigen zeitlichen Veränderungen zwischen den beiden Gemeinschaften. Die Alpha-Indices Shannon und Inverse Simpson zeigten Trends, die darauf hindeuten, dass sich die kleine Fraktion im Laufe der Zeit von einer durch wenige Taxa dominierten Gemeinschaft zu einer gleichmäßiger verteilten entwickelte. Im Gegensatz dazu wurde die große Fraktion gegen Ende des Monats ungleichmäßiger, da einzelne Taxa in ihren relativen Anteilen zunahmen. Eine Analyse des zeitlichen Turnovers bestätigte diese Verschiebungen, wobei Jaccard-Werte von 0.56 bis 0.62 einen moderaten Austausch von Taxa in beiden Fraktionen im Verlauf des Julis widerspiegelten.

Die Analyse der Umweltfaktoren ergab, dass Nitrit signifikant mit der großen Fraktion korrelierte, während gelöster Sauerstoff und Nitrit mit der kleinen Fraktion assoziiert waren. Zusammenfassend unterstreichen diese Ergebnisse die dynamische Natur der Protistengemeinschaft im Greifswalder Bodden und verdeutlichen, dass sowohl kurzzeitige Veränderungen als auch Korrelationen mit Umweltparametern größenspezifisch variieren können.

1. Introduction

1.1 Ecological Role of Marine Protists

The oceans cover up to 71% of the Earth's surface (Charette & Smith, 2010) and are home to diverse ecosystems, including crucial habitats for protists. As predominantly single-celled, microscopic, eukaryotic organisms (Adl et al., 2005), classically encompassing the algae, protozoa, and fungal-like forms (Corliss, 2002), protists are key components of global marine ecosystems. Microbial eukaryotic protists are thought to account for a substantial proportion of global biodiversity (Pawlowski et al., 2012; De Vargas et al., 2015), yet they remain poorly understood (Adl et al., 2019; Pawlowski et al., 2012).

Serving as the foundation of aquatic food webs, protists play a vital role in biogeochemical cycles (Legendre & Le Fèvre, 1995). Acting among other things as photoautotrophic primary producers (Corliss, 2002), phytoplankton account for approximately 46% of global primary production (Field et al., 1998), thereby driving aquatic carbon fixation. However, their metabolic versatility extends beyond pure autotrophy: many protists acquire photosynthetic capacity through endosymbiosis or organelle retention, a widespread yet frequently underestimated strategy (Stoecker et al., 2009), while heterotrophic and mixotrophic forms act as bacterivores and grazers, linking microbial production to higher trophic levels via the microbial loop (Mitra et al., 2014).

Adding to this metabolic diversity, parasitism stands out as one of the most successful life strategies in nature. It is estimated that roughly half of all species on Earth are parasitic (Skovgaard, 2014). In marine planktonic ecosystems, the majority of these parasites are themselves protists. Their hosts include a wide range of organisms, from other protists like dinoflagellates and diatoms to larger invertebrates (Skovgaard, 2014). Key representatives of parasitic protists include fungal parasites, specifically chytrids, which are recognized as vital regulators of phytoplankton populations (Skovgaard, 2014). Furthermore, marine alveolates such as Syndiniales frequently dominate marine communities (Massana, 2011; Worden et al., 2015), infecting other dinoflagellates and various other protists (Skovgaard, 2014). This parasitic pathway within the marine food web facilitates the transfer of energy from large hosts to smaller consumers. By doing so, it significantly shapes the structure of planktonic communities.

As key components of marine food webs and biogeochemical cycles, microbial eukaryotes are able to significantly influence marine ecosystem dynamics, making it essential to understand how these communities are structured and function. Traditionally, protist communities were characterized primarily using microscopy, which is time-consuming and requires considerable taxonomic expertise for morphological identification. With the advent of environmental DNA (eDNA) metabarcoding approaches, it has become possible to identify a larger number of protist species more rapidly and to discover previously unknown diversity (De Vargas et al., 2015; Bálint et al., 2018; Sildever et al., 2021; Andersson et al., 2023; Salis & Hansson, 2025). The increased application of these molecular methods has significantly advanced our understanding of microbial eukaryotic diversity and led to major revisions in taxonomic classification (Pawlowski et al., 2012; De Vargas et al., 2015; Adl et al., 2019). Studies have shown that the true diversity of protist groups is considerably greater than previously described based on microscopy alone, yet knowledge gaps remain, as molecular studies targeting the full microbial eukaryotic community are still less common than those focusing on prokaryotes (Mazur-Marzec et al., 2024). In particular, microscopy reaches its detection limits, especially when applied to pico- and nanoplankton, due to their small cell size and morphological similarity between taxa, what metabarcoding approaches can effectively resolve, making ecologically important and cryptic taxa visible (Mazur-Marzec et al., 2024).

1.2 Size-Fractionated Communities and Ecological Niche Partitioning

For a more detailed insight into the microbial eukaryotic community, various studies have shown that it is useful to separate the community according to size using different filter sizes (Rojas-Jimenez et al., 2019; Grattepanche et al., 2022; Blais et al., 2024; Fournier et al., 2024; Froján et al., 2025). Cell size of coastal water plankton has been identified as a key trait with different patterns correlating with the environment (Wu & Liu, 2022), as differences in cell size are closely linked to ecological strategies and resource utilization, making it important to consider the size fractions separately in order to obtain a more accurate picture. Zheng et al. (2025) found that cell size is associated with niche breadth. Smaller cells, such as pico-protists (0.2–2 μm), tend to occupy broader ecological niches than larger cells, suggesting that larger size fractions have a more limited capacity to adapt to varying environmental conditions. Feeding type can also vary with cell size: smaller protists were predominantly characterized by parasitic taxa such as Syndiniales, whereas larger protists were primarily mixotrophic or symbiotic (Zheng et al., 2025).

There are various approaches to define the size fractions. Some studies (Corrales-Ugalde et al., 2025; Froján et al., 2025; Gorokhova & Zinchenko, 2025; L. Wang et al., 2026) refer to the classification of plankton according to Sieburth et al. (1978), which primarily uses the size fractions macroplankton (>200 µm), microplankton (20–200 µm), nanoplankton (2–20 µm), and picoplankton (0.2–2 µm). However, as other studies adopt different size ranges, it appears that these boundaries are not strictly fixed and often tend to overlap across the literature (Z. Xu et al., 2018; Rojas-Jimenez et al., 2019; L. J. Clarke & Deagle, 2020; Grattepanche et al., 2022; Wu & Liu, 2022; Blais et al., 2024; Fournier et al., 2024; Sassenhagen et al., 2025). In this study, the microbial eukaryote community was divided into ≥5 µm (hereinafter referred to as nanoplankton or large fraction) and 0.22–5 µm (hereinafter referred to as picoplankton or small fraction). It should be noted that since the ≥5 µm fraction has no upper size limit, it inherently includes microplankton-sized organisms; however, for simplicity, this fraction is referred to as nanoplankton throughout this study.

1.3 Environmental Drivers and Community Dynamics: From the Baltic Sea to the Greifswalder Bodden

Brackish waters act as transition zones between freshwater and marine systems (Cognetti & Maltagliati, 2000; Müller et al., 2010). They are home to a unique diversity of organisms, ranging from stenohaline freshwater organisms to euryhaline taxa. This mixed community is ecologically distinct, but it is also sensitive to environmental changes. The pronounced salinity gradient in these areas can shift both spatially and temporally, acting as a major abiotic driver structuring aquatic communities (Telesh et al., 2013).

In the Baltic Sea, salinity varies geographically: the western regions are predominantly saltwater-brackish (10–30 PSU), the central basin is primarily brackish (5–7 PSU), and the eastern and northern areas transition to freshwater-brackish conditions (0–6 PSU; Herlemann et al., 2011). Along this gradient, both the diversity and composition of microbial eukaryotic communities shift considerably and dominant functional groups differ across the gradient (Olofsson et al., 2020). Their seasonal dynamics also vary: at higher salinities (20–30 PSU), cell abundance peaks in early spring, whereas at lower salinities (0–10 PSU), peak abundances occur between spring and summer (Olofsson et al., 2020). A well-known concept describing how organisms depend on salinity is the species minimum, which occurs at 5–8 PSU (Cognetti & Maltagliati, 2000; Müller et al., 2010; Telesh et al., 2011, 2013). According to Remane's classic model (1934), biodiversity drops in this specific range because neither marine nor

freshwater species are optimally adapted to these conditions. Interestingly, planktonic protists seem to follow the opposite trend: Telesh et al. (2011, 2013) described a ‘paradoxical’ diversity maximum for microbial eukaryotes in this salinity range, which points to the existence of specialized, autochthonous brackish water communities.

Temperature is one of the most influential drivers of protist community dynamics. It directly affects biochemical and cellular processes, and thus the metabolic performance and competitive ability of individual taxa (Jänes et al., 2017). Rising temperatures, as a consequence of global climate change, are already altering aquatic ecosystems worldwide (Calvin et al., 2023). In the Baltic Sea, warming promotes stronger water column stratification, which shifts competitive advantages toward motile, stratification-tolerant taxa, while potentially disadvantaging groups that thrive under well-mixed, nutrient-rich conditions (Tozzi et al., 2004; Moore et al., 2008; Klais et al., 2011). Picoplankton, in particular, can respond rapidly to changes in environmental conditions, as demonstrated by pronounced diel variability in growth (Vaulot & Marie, 1999). The annual mean water surface temperature is higher in the south of the Baltic Sea than in the north (Siegel et al., 2006), and warmer conditions, combined with increased water column stratification, can alter the competitive balance between different protist groups (Gasiūnaitė et al., 2005). More broadly, temperature-driven stratification affects nutrient availability and light regimes, thereby influencing the entire protist community.

Since they are often located near densely populated coasts, brackish systems face strong anthropogenic pressure (Müller et al., 2010). This includes eutrophication from nutrient and pollutant runoff, intensive fishing, tourism, and habitat changes driven by industry and shipping. The Baltic Sea is a prime example: it is one of the world's largest coastal brackish systems (Telesh et al., 2013). Factors like the long water residence time (>20 years) and minimal tidal action further shape the system's unique dynamics. Due to this intense human influence, the Baltic Sea has shifted toward a eutrophic state, which has fundamentally altered the plankton communities (Halpern et al., 2008; Klais et al., 2013; NOAA, 2024). Since 1989, for example, diatoms in the southern Baltic’s spring bloom have declined, while dinoflagellates have increased (Wasmund et al., 1998). This shift is likely linked to rising winter temperatures and stronger stratification of the water column, both clear signals of climate change (Klais et al., 2013). Building on the eutrophic conditions already established in systems such as the Baltic Sea, elevated nutrient availability can shift competitive balances between protist groups (Bi et al., 2021; Hallegraeff et al., 2003).

One expression of these community dynamics are phytoplankton blooms, which represent extreme growth events involving one or more species and can significantly impact entire aquatic ecosystems (D. M. Anderson et al., 2002; Hallegraeff, 2010). While blooms are a natural feature of productive coastal systems, their frequency and intensity can increase under eutrophic conditions and elevated temperatures (Davidson et al., 2014). Such bloom events can alter nutrient cycling, affect light availability for benthic organisms (Moore et al., 2008; Berdalet et al., 2016), and propagate through the food web via grazing interactions (Cloern, 1996) – underscoring the broader ecological significance of protist community composition. Consequently, the early detection and mechanical understanding of these blooms are crucial for predicting their ecological impacts and developing management strategies for coastal protection.

In summary, microbial eukaryotic communities are shaped by a complex interplay of abiotic and biotic factors, the exact mechanisms of which are still not fully understood. Beyond drivers like temperature and nutrient availability, other key influences include light, pH, predation, and physical forcing, such as wind-driven mixing and currents. Crucially, these factors rarely act in isolation (Fu et al., 2012; Griffith & Gobler, 2020; Hallegraeff, 2010; Klais et al., 2011), as species in nature often respond differently to combinations of stressors than to individual ones (Fredersdorf et al., 2009). Their interactions determine species boundaries and can facilitate the establishment of taxa in previously unsuitable niches (Jänes et al., 2017; Viitasalo & Bonsdorff, 2022), making it difficult to attribute community change to any single driver. This is particularly evident with salinity fluctuations, which, when driven by episodic freshwater inflows, can trigger rapid community shifts by favoring osmotically tolerant taxa (Fu et al., 2012). Furthermore, while the composition of pico- and nanoplanktonic protists is strongly structured by the combined effects of salinity, temperature, and nutrients (Piwosz et al., 2018), research addressing these effects on the full microbial eukaryotic community, especially regarding short-term responses, remains insufficient (Slaveykova et al., 2016), highlighting a critical gap in our current understanding.

The Greifswalder Bodden (GWB) sits within a salinity range of 5–12 PSU and has limited water exchange with the open Baltic (Schiewer, 2001). As a shallow, semi-enclosed system, it serves as a sensitive indicator for environmental change, where rapid fluctuations can trigger immediate biological responses. High nutrient loads in the mid-to-late 20th century triggered a regime shift here, moving from a macrophyte-dominated to a phytoplankton-dominated ecosystem (Munkes, 2005; Schiewer, 2008). This has completely changed the dynamics and

structure of the microbial community. Because the GWB is shallow, it is also prone to sediment resuspension caused by wind and currents. Sassenhagen et al. (2025) showed that the resuspension, along with benthic resting stages, can significantly influence the composition of microbial eukaryotes. However, while some insights into general seasonal trends in the GWB exist, short-term temporal variation in protist community composition remains poorly understood.

1.4 Research Objectives and Hypotheses

The aim of this study is to investigate short-term temporal variation in microbial eukaryotic community composition using 18S rRNA metabarcoding data and to explore the potential influence of environmental parameters on community structure. To address this aim, the following research question and hypotheses were formulated:

Research Question: Does the microbial eukaryotic community composition vary across short-term temporal scales, do these patterns differ between size fractions, and to what extent are these patterns associated with environmental conditions?

Hypothesis 1: The microbial eukaryotic community composition differs among sampling weeks, indicating short-term temporal turnover.

Hypothesis 2: The two size fractions (≥5 µm and 0.22–5 µm) differ in community composition and show distinct temporal succession dynamics.

Hypothesis 3: Environmental variables such as temperature and nutrient concentrations are associated with community compositional patterns.

2. Materials and Methods

2.1 Sampling

2.1.1 Study Site

The study site was in the Greifswalder Bodden (GWB), Germany, a large, shallow bay on the southern coast of the Baltic Sea (Figure 1) with a surface area of 494 km^2 (Landesamt für Umwelt, Naturschutz und Geologie, n.d.). It has two connections to the Baltic Sea: a large opening to the east and a small opening to the west, known as the Strelasund. The Bodden averages 5.8 meters in depth and reaches a maximum depth of 13.5 meters in the east (Schiewer, 2008). The sediment varies between mud, sand, and clay in different parts of the GWB (Lampe, 2022). Parameters such as salinity and temperature fluctuate greatly. Salinity ranges from 5.3 to 12.2 PSU, with an average of 7.4 (Schiewer, 2008), reflecting the strong gradient between freshwater inflows and exchange with the Baltic Sea. Water temperatures vary seasonally from approximately 3 °C to 25 °C (Schiewer, 2008).

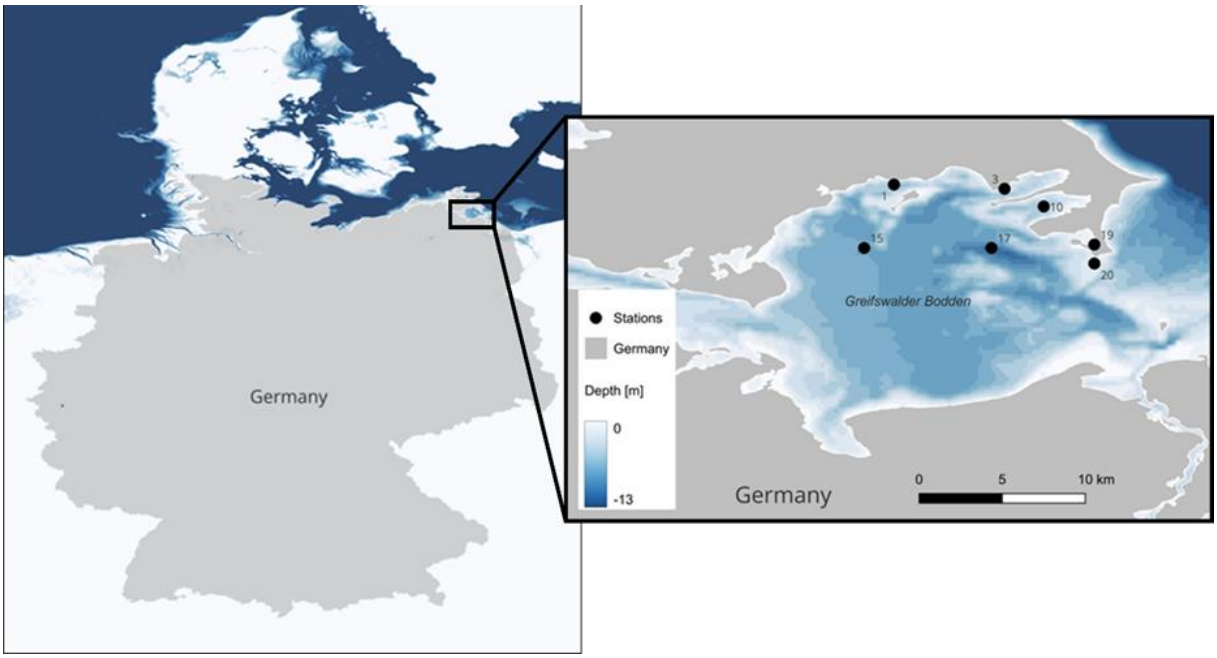

Figure 1: Study area and sampling locations. (Left) Map of Germany highlighting the Greifswalder Bodden (black square). (Right) Detailed map of the Greifswalder Bodden including the sampling stations 1, 3, 10, 15, 17, 19 and 20 (black dots). Water at various depths is shown in blue (from white (0 m depth) to dark blue (13 m depth and deeper). Germany and the German islands are colored gray. The map was created using QGIS.

Water circulates and exchanges with the open Baltic Sea seasonally, peaking in March (Bauer et al., 2013). In general, inflow and outflow events are relatively short, averaging five hours,

despite the relatively high and constant exchange rate. Because it is wind-driven, the direction of the current changes rapidly, causing the water in the GWB to oscillate at the inflows and outflows. This ultimately means that the actual water exchange is probably lower, as the same water masses remain at the inflows and outflows (Bauer et al., 2013).

Figure 1 shows a map created using QGIS (v3.40.3). Data from GADM (version 4.1) was used for the German national borders (GADM, 2022) and the 'GEBCO 2024: Sub-Ice Topography/Bathymetry' dataset (GEBCO Bathymetric Compilation Group 2024, 2024) for the bathymetry. Sampling was carried out at seven stations in the GB, which were selected to cover different areas of the Bodden, including coastal areas, more central basin areas, and regions with greater water exchange with the open Baltic Sea. This spatial distribution of stations was intended to capture potential differences in physical and chemical conditions and their influence on the microbial eukaryotic community.

2.1.2 Sample Collection

The study period covered a full month, July 2025. Water samples were taken twice a week at seven different stations (Figure 1) and environmental parameters were measured. The German Federal Agency for Nature Conservation (BfN/ Bundesamt für Naturschutz) provided the boat ‘Gavia’ (FASTER 650 Cat) and boat operators for every sampling day. At each station, a Conductivity–Temperature–Depth (CTD) profiler (Sea & Sun Technology GmbH, Germany) was used, a water sample was taken with a manual 2 L Niskin bottle at a depth of one meter and the visual depth was measured with a Secchi disk. Samples were taken on a total of 8 different days. The geographical coordinates of these stations can be found in Table 1. Samples from stations 3 and 19 were collected from the pier and from all other stations from the boat.

Table 1: Overview of sampling stations in the Greifswalder Bodden, including geographic coordinates (latitude, longitude).

Sampling Stations	Latitude	Longitude
1	54.336180	13.522574
3	54.332210	13.624652
10	54.315896	13.660823
15	54.277452	13.495023
17	54.277452	13.612553
19	54.280598	13.707564
20	54.263020	13.707564

2.1.3 Water Sample Filtration and Sample Processing

In the laboratory, 1 L of each water sample was filtered directly after sampling for the following DNA extraction using a 5 µm mixed cellulose esters (MCE) membrane filters (Ø 47 mm, MF-Millipore™ Membrane Filters, Merck Millipore, Tullagreen, Carrigtwohill, Co. Cork, Ireland) and the filtered was subsequently passed through 0.22 µm MCE membrane filters (Ø 47 mm, MF-Millipore™ Membrane Filters, Merck Millipore, Tullagreen, Carrigtwohill, Co. Cork, Ireland). Filtration was performed under vacuum using a diaphragm pump (KNF Neuberger, model N 026.1.2AN.18, Freiburg, Germany). Additionally, 500 mL water from each sample was filtered onto GF/F glass microfiber filters (Ø 47 mm, Whatman™ GF/F, GE Healthcare UK Limited, Amersham Place, Little Chalfont, Buckinghamshire HP7 9NA, United Kingdom) for chlorophyll *a* (Chl *a*) measurements. Chl *a* was measured according to HELCOM (n.d.) and using a 10-AU Fluorometer (NORDANTEC GmbH, Bremerhaven, Germany). The filters were stored at -20 °C. Finally, 15 mL of the 0.22 µm filtrate were transferred into a 15 mL Falcon tube (polypropylene tube) and stored at -20 °C for dissolved nutrient analyses. Nutrients were measured colorimetrically according to Grasshoff et al. (2009) by means of a Seal Analytical QuAAtro39 continuous flow analyzer.

2.2 DNA Extraction and Sequencing

DNA retained on the 5 µm and 0.22 µm MCE membrane filters was extracted using the DNeasy PowerWater Kit (Qiagen, Germany), following the manufacturer's protocol with the following modifications: the filter was placed directly into the bead tube, rather than being rolled, and cut with sterile scissors; bead beating was performed using an MP FastPrep®-24 5G bead beating grinder and lysis system (bead beating is performed twice, each time for 45 seconds, with a five min break in between); and elution involved the addition of 50 µL of EB buffer twice (2 × 50 µL = 100 µL in total), followed by a 2 min incubation prior to centrifugation. The DNA content was determined using a fluorescence-based assay on a Qubit™ 4 Fluorometer (Invitrogen, Thermo Fisher Scientific) with the Qubit™ dsDNA BR Assay, and the purity was assessed using a Thermo Scientific™ NanoDrop™ One spectrophotometer (Thermo Fisher Scientific) with an A260/280 absorbance of 1.8–2.0, which indicates relatively pure DNA. A total of 50 µL of each DNA extract was sent to Biomarker Technologies (BMK GmbH, Münster, Germany) for library preparation and amplicon sequencing. The 18S rRNA V4 region was amplified using the forward primer TAReuk454FWD1 (5'-CCAGCASCYGCGGTAATTCC-3') and the reverse primer TAReukREV3 (5'-ACTTTCGTTCTTGATYRA-3') originally

described by Stoeck et al. (2010), followed by paired-end sequencing (2 × 150 bp) on an Illumina NovaSeq 6000 platform. Demultiplexed, adapter-clipped, paired-end FASTQ files were provided.

2.3 Physicochemical Data Processing

CTD profiles were recorded using the Standard Data Acquisition software (SDA, © T. Finger, 1999–2018, Sea & Sun Technology) and stored as TOB files. Downcast data were processed in the R environment (R Core Team, 2025; v4.5.1) using tidyverse (Wickham et al., 2019; v2.0.0); physical and chemical parameters were extracted at 1 m depth via linear interpolation between adjacent pressure readings (target: 1.0 dbar, window: ± 0.15 dbar) and matched to the corresponding water samples by station and date.

2.4 Bioinformatics

The demultiplexed paired-end reads were processed using an in-house Snakemake (Köster, 2024) based workflow (Hassenrück, 2022; following the DADA2 pipeline by Callahan et al., 2016). The workflow uses GNU Parallel (Tange, 2011) for parallel execution. Primers were removed using cutadapt (Martin, 2011; v4.9), allowing an error rate of 0.16. Forward reads were trimmed to 230 bp and reverse reads to 225 bp; all reads with more than the expected errors (maxEE_R1 = 1, maxEE_R2 = 2) were discarded. Error rate models for forward and backward reads were derived using learnErrors(), applying a custom Locally Estimated Scatterplot Smoothing (loess)-based error function for binned quality scores according to the specification errfun = “2,11,25,37”. Denoising was conducted using dada(..., pool = “pseudo”) to increase sensitivity to low-abundance sequence variants across samples, while preventing the inflation of false positives. Forward and reverse denoised reads were subsequently merged, allowing no mismatches in the overlap region (minimum 10bp). Merged reads were compiled into an amplicon sequence variant (ASV) table using makeSequenceTable(). Chimeric sequences were identified and removed using removeBimeraDenovo(method = “consensus”). Based on the expected amplificon size, all reads with a length outside the range of 300 to 460 bp were discarded to ensure the removal of non-specific amplification products.

Taxonomic assignment was performed using DADA2’s assignTaxonomy() naïve Bayesian classifier against the Protist Ribosomal Database (PR2 v5.1.0; Vaulot et al., 2025) 18S reference

database with a bootstrap cutoff of 70. Only ASVs assigned to the domain Eukaryota were retained for downstream analyses.

2.4.1 Community Analysis and Statistical Methods

All ecological and statistical analyses were performed in the R environment (R Core Team, 2025; v4.5.1). Metabarcoding data were organized and processed using phyloseq (McMurdie & Holmes, 2013; v1.52.0), with data processing performed using dplyr (Wickham et al., 2023; v1.1.4). Community ecology analyses were performed using vegan (Oksanen et al., 2025; v2.7-2). Visualizations were created using the ggplot2 package (Wickham, 2016; v4.0.0) and, if necessary, combined with patchwork (Pedersen, 2025; v1.3.2) to create composite images.

ASV counts, taxonomy tables, and sequences were imported and merged into a phyloseq object. Metadata were added and to focus on microeukaryotic plankton, unclassified eukaryotes, metazoans, and streptophytes were removed.

Sequence depth was assessed using rarefaction curves (rarecurve(), vegan). Visual observation of curves approaching saturation was verified by a quantitative slope analysis to ensure adequate coverage of microbial diversity. Consequently, the non-rarefied dataset was considered suitable for all downstream community analyses, avoiding the loss of information associated with traditional rarefying.

For visualization and description of community dynamics, ASV tables were aggregated at class and genus level using tax_glom(). In contrast, all diversity and multivariate analyses were performed at the ASV level to maintain maximum biological resolution. In order to account for the different ecological niches and potentially divergent succession dynamics of the differently sized microbial eukaryotic communities, two sub-datasets were created for diversity analysis, one for each size fraction (≥5 and 0.22–5 µm). For multivariate analyses, the dataset was reduced to samples with complete environmental metadata; samples with missing values were excluded, resulting in a final dataset.

Sequencing depth was assessed by summarizing total reads per sample and testing for systematic differences across sampling weeks and size fractions using Kruskal-Wallis tests (R base package). The potential bias of sequencing depth on observed ASV richness was evaluated using Spearman's rank correlation (R base package, stats).

Alpha diversity metrics (Observed Richness, Shannon, Inverse Simpson) were calculated using estimate_richness in the phyloseq package. Shannon and Inverse Simpson indices were additionally calculated as diversity metrics less sensitive to sequencing depth. Linear Mixed Models (LMM) were employed using lme4 (Bates et al., 2015; v1.1.38) for the Shannon and Inverse Simpson indices. For Observed ASV Richness, a Generalized Linear Mixed Model (GLMM) with a Negative Binomial distribution was employed using glmmTMB (Brooks et al., 2017; v1.1.14) because it provided a better overall fit than the corresponding Poisson model. To account for variation in sequencing depth, the log-transformed total read count per sample was included as a covariate in the GLMM. To reflect the repeated measures design, Sampling Week and Size Fraction were included as fixed effects. Water Sample, defined as the unique combination of sampling station and collection date from which both size fractions were derived, was included as a random effect to account for the paired nature of the samples. The significance of fixed effects and their interactions was evaluated using Type III Wald Chi-Square tests. Model assumptions were assessed using simulated-residual diagnostics implemented in the DHARMa package (Hartig et al., 2024; v0.4.7), including visual inspection of Q-Q plots and tests for uniformity and homogeneity of variance. Given the significant interaction between Sampling Week and Size Fraction, post-hoc comparisons were conducted using estimated marginal means (emmeans; Lenth et al., 2026; v2.0.1) with Benjamini-Hochberg (FDR) correction.

For beta diversity analysis, ASV count data were converted to relative abundances to account for differences in sequencing depth. Bray-Curtis dissimilarities were calculated based on these relative abundances to assess community compositional differences. This metric was chosen as it incorporates abundance information and is robust to the high sparsity typical of ASV count data, making it widely used in microbial community ecology. The community structure was visualized using non-metric multidimensional scaling (NMDS), examining both global clustering and subsets of the two size fractions. Statistical differences in community composition were assessed using PERMANOVA (adonis2), analyzing the sampling week (as a categorical factor), the size fraction, and their interaction. Within each size fraction, temporal differences were additionally assessed using ANOSIM, with station as strata, to provide an interpretable effect size (*R*-value) for the strength of temporal separation. To assess the reliability of these results, multivariate homogeneity of group dispersions was tested using BETADISPER. All analyses were based on 999 permutations with a fixed random seed (set.seed(42)) to ensure reproducibility. In accordance with the study design, permutation schemes were specifically constrained: for comparisons over time, station was used as a

blocking factor to account for repeated measures. The effect of station on community structure was additionally tested in a separate PERMANOVA model with sampling week as blocking factor. For comparisons between size fractions, permutations were restricted within each individual water sample to account for the paired nature of the filters. An exception was the global PERMANOVA, where station was used as the sole blocking factor, as the permutation framework (adonis2) only allows for a single blocking structure per model, preventing the simultaneous application of multiple nested restrictions for main effects and their interaction.

To quantify the temporal change in the communities, the Bray-Curtis dissimilarities (abundance-based) and the Jaccard index (presence/absence) between consecutive weeks were calculated. All samples were first converted to relative abundances to account for differences in sequencing depth between samples. Within each week, relative abundances were averaged across replicate sampling events per station prior to dissimilarity calculation, to account for uneven sampling effort within weeks. For each station and size fraction, pairwise dissimilarities were then calculated between the resulting weekly mean profiles of consecutive weeks, retaining only inter-week transitions (W1-W2, W2-W3, W3-W4). While the Bray-Curtis dissimilarity captures structural shifts in dominance patterns, the Jaccard index reflects actual taxonomic turnover based on presence and absence of ASVs. The resulting values were visualized as box plots showing the full distribution across stations, and summarized as means ± standard error (SE) for reporting.

Multicollinearity among environmental predictors was assessed using variance inflation factors (VIF); all variables returned VIF values below 3 (Table S 7), with the exception of chlorophyll *a* (VIF = 3.05), which marginally exceeded this threshold but was retained as it showed no critical collinearity (Zuur et al., 2010). The possible correlation of environmental parameters with community structure was analyzed separately for each size fraction using vector fitting (envfit), with station as a blocking factor to account for the repeated measures structure. Only significant vectors ($p < 0.05$) were visualized in the ordination. Additionally, PERMANOVA (adonis2) was applied to test for significant effects of environmental variables on community composition, using station as a blocking factor and marginal testing (by = "margin") with 999 permutations. A fixed random seed (set.seed(42)) was used throughout to ensure reproducibility.

In order to explore the community composition and its temporal dynamics, the 20 most dominant taxa (at class and genus level, respectively; taxonomic labels reflect PR2 database annotations at the respective rank) were identified based on cumulative relative abundance

across all samples and size fractions, and visualized per size fraction and station in stacked area charts (using phyloseq and ggplot2 to transform the data into relative abundances) over the sampling period (July), with the x-axis reflecting actual sampling dates labeled by week (W1–W4). All other groups were grouped under 'Other'.

3. Results

3.1 Sequencing Summary and Data Quality

3.1.1 Sequencing Statistics and Taxonomic Filtering

The dataset comprised a total of 114 samples, which were divided into two size fractions: the larger (≥5 µm, n = 57 samples) and the smaller (0.22–5 µm, n = 57 samples). To account for the different ecological niches and potentially divergent succession dynamics of microbial communities of different sizes, the dataset divided into size fractions was used for several diversity analyses. The sequence length distribution before filtering can be seen in Figure S 1. There was a total of 8,153 ASVs.

First, unclassified eukaryotes were eliminated, resulting in the removal of 839 ASVs. Subsequently, another 1,432 ASVs were eliminated as Metazoa and Streptophyta were filtered out. After taxonomic filtering, 6,721 ASVs remained, with a sequence length ranging from 300 to 443 bp (mean of 380.3 bp, median 381 bp) (Figure S 2). The number of reads per sample ranged from 41,783 to 182,586. Sequencing depth did not differ significantly between size fractions (Kruskal-Wallis, $X^2 = 1.77$, $df = 1$, $p = 0.184$), but varied significantly across sampling weeks ($X^2 = 12.23$, $df = 3$, $p = 0.007$). A weak positive correlation between sequencing depth and observed ASV richness was detected (Spearman's $\rho = 0.24$, $p = 0.009$; Figure S 4).

3.1.2 Rarefaction and Quantitative Slope Analysis

Rarefaction curves were created to evaluate the sequencing depth. The visual inspections of the rarefaction curves (Figure S 3) showed that the sequencing depth was sufficient to capture most of the taxonomic diversity of the samples, as most curves reached the saturation phase (plateau). The total number of reads across all samples was 4,763,262.

Visual observation was verified and confirmed by a quantitative slope analysis. The discovery of new ASVs across all samples had an average rate of 0.544 new ASVs per 1,000 additional reads, suggesting that the sequencing depth was sufficient to capture the comprehensive microbial diversity. Samples with high sequencing depth (e.g., B45, B42) showed near-complete saturation with less than 0.11 new ASVs per 1,000 reads (Table S 1).

Even samples with the steepest remaining slopes (e.g., A44, A53) yielded only about 1.25 to 1.41 new ASVs per 1,000 reads (Table S 2), suggesting that further sequencing would not significantly alter the observed community structure. Consequently, the dataset was considered suitable for downstream diversity analyses.

3.1.3 Sample Retention and Metadata Quality

The ASVs were aggregated at genus and class levels, resulting in 892 unique genera and 132 unique classes. A summary of the taxonomic counts can be seen in Table 2.

Table 2: Summary of sequencing depth and taxonomic subset counts. The table provides an overview of sequencing depth and taxonomic richness (ASVs, Genera, and Classes) for the full dataset and specific size-fraction subsets. Taxonomic subset counts are differentiated between the large (≥5 µm) and small (0.22-5 µm) fractions.

	Total	≥5 µm Size Fraction	0.22–5 µm Size Fraction
Reads	11,813,045	5,692,682	6,120,363
ASVs	6,721	5,006	3,637
Genera	892	775	715
Classes	132	119	119

For multivariate environmental analyses, all samples were filtered to ensure complete environmental metadata for nine key variables. Secchi depth was excluded from the analysis prior to filtering due to significant data gaps (17.5% missing values, Table S 3). After filtering for complete environmental data, 102 samples (51 per size fraction) were retained for subsequent multivariate analyses, corresponding to a retention rate of 89.5%. A total of 12 samples (6 per size fraction) were excluded due to incomplete environmental metadata, resulting in the removal of 296 ASVs that were exclusively present in the excluded samples. The final dataset used for environmental modeling comprised 6,425 ASVs, with the excluded reads accounting for 9.27% of total filtered reads.

3.2 Alpha Diversity Patterns

3.2.1 Influence of Size Fraction on Diversity and Evenness

Alpha diversity metrics were calculated for each sample to compare the microbial community structures between the two size fractions (Table 3). The mean richness of the large fraction was 657 (± 132 SD (standard deviation)), mean Shannon index was 3.96 (± 0.27 SD) and mean Inverse Simpson index was 20.90 (± 6.41 SD). In contrast, the smaller size fraction had means of 450 (± 115 SD), 3.50 (± 0.48 SD) and 15.30 (± 7.80 SD), respectively. The larger fraction shows less variation over the study period, as the SD of the Shannon index for the larger fraction is 0.27, whereas the standard deviation for the smaller fraction is 0.48.

Table 3: Descriptive statistics of alpha diversity indices by size fraction. Shown are the mean values (± standard deviation, SD) and standard error (SE) for observed ASV richness, the Shannon index, and the inverse Simpson index. The values are listed separately for the large fraction (≥5 µm) and the small fraction (0.22-5 µm).

	Size Fraction	Mean ± SD	SE
Observed ASV Richness	≥5 µm	657 ± 132	17.50
	0.22-5 µm	450 ± 115	15.30
Shannon Index	≥5 µm	3.96 ± 0.27	0.04
	0.22-5 µm	3.50 ± 0.48	0.06
Inverse Simpson Index	≥5 µm	20.90 ± 6.41	0.85
	0.22-5 µm	15.30 ± 7.80	1.03

3.2.2 Temporal Dynamics of Alpha Diversity throughout July

The temporal development within the smaller fraction was particularly striking (Figure 2). Diversity increased continuously over the four-week period, indicating increasing complexity and a more balanced species distribution (evenness). In both fractions, observed ASV richness increased throughout July, remaining consistently higher in the larger fraction. Though there was a slight decline in week four in the Shannon and inverse Simpson indices, the estimated richness remained stable and above that of the smaller fraction.

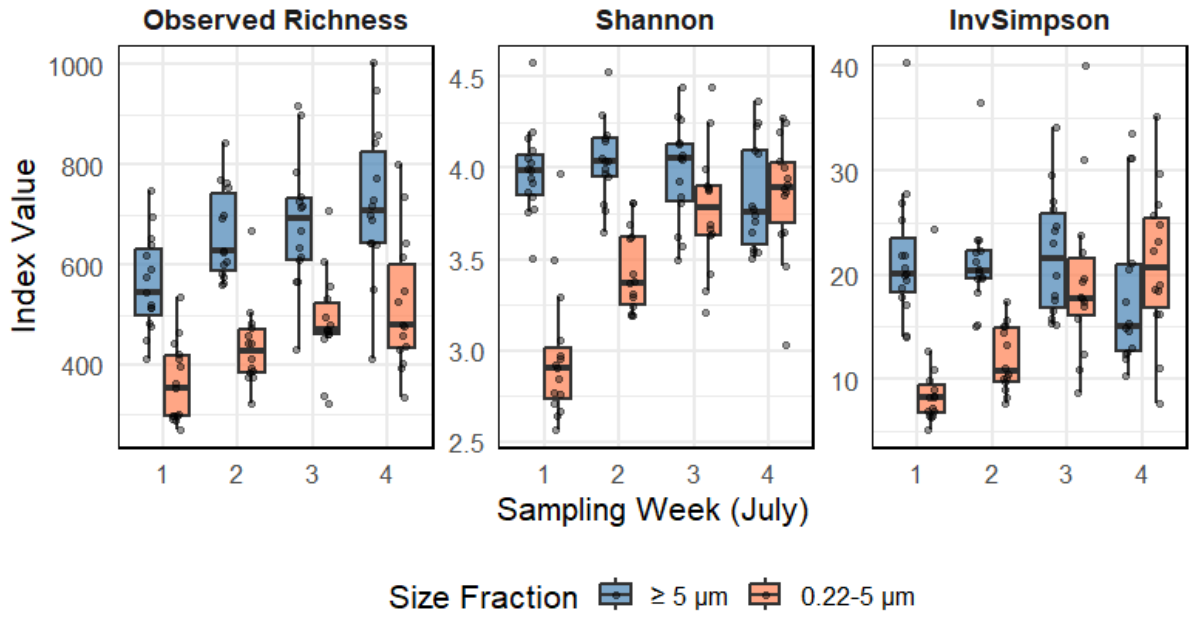

Figure 2: Alpha diversity of microbial communities over the sampling period. The diversity is divided into the size fractions ≥5 µm (blue) and 0.22-5 µm (orange) over a period of four weeks in July 2025. The panels present the observed ASV richness, the Shannon index, and the inverse Simpson index. The box plots are used to indicate the median and the upper and lower quartiles; the individual measurements are plotted as dots above the boxes to illustrate the data dispersion. The points have been slightly offset to avoid overlap between points with identical values.

The residual diagnostics showed good model fit for the Observed Richness, Shannon and Inverse Simpson indices (Figure S 5, Figure S 6, Figure S 7). In addition, there was a significant interaction between sampling week and size fraction (Table 4), which is why the differences within each fraction were interpreted between sampling weeks.

Table 4: Model Output – Type III Analysis (Overall Effects). Statistical results for the influence of sampling week (Week), size fraction (Fraction), and their interaction on microbial diversity indices (Observed ASV Richness, Shannon Index, and Inverse Simpson Index). Wald Chi-Square tests (X^2) are reported. Note: For LMMs, the degrees of freedom (*df*) were calculated using the Satterthwaite approximation. Significance levels: *** $p < 0.001$; ** $p < 0.01$; * $p < 0.05$; ns: not significant ($p > 0.05$).

Index	Factor	X^2	*df*	*p*
Observed Richness (GLMM)	Week	6.71	3	0.082
	Fraction	113.27	1	**< 0.001*** **
	Week × Fraction	9.48	3	**0.024***
Shannon Index (LMM)	Week	3.35	3	0.341 (ns)
	Fraction	92.15	1	**< 0.001*** **
	Week × Fraction	53.34	3	**< 0.001*** **
Inverse Simpson (LMM)	Week	2.61	3	0.455 (ns)
	Fraction	32.72	1	**< 0.001*** **
	Week × Fraction	27.31	3	**< 0.001*** **

The random effect of station explained little to no additional variance across all alpha diversity models (Table S 4), suggesting that differences among sampling sites were negligible relative to temporal and size-fraction effects. Water sample, by contrast, captured meaningful residual variance for Inverse Simpson, confirming the importance of accounting for the paired sample structure.

Post-hoc comparisons showed distinct temporal trajectories for the two size fractions. In the small fraction (0.22-5 µm), the Shannon index increased significantly from week 1 to week 3 (Table 5, all $p < 0.01$), followed by a plateau with no further significant changes towards week 4 ($p = 0.459$). Observed ASV richness showed an initial increase from week 1 to week 2 ($p = 0.0.3$), but no significant differences were detected between the subsequent weeks (W2 – W3 and W3 – W4, $p > 0.05$). The inverse Simpson index followed a similar trend to the Shannon index, although the initial increase between week 1 and week 2 was not significant ($p = 0.281$). In contrast, the large fraction (≥5 µm) exhibited a different pattern (Table S 5). No significant differences were observed for Observed ASV richness, Shannon and inverse Simpson indices in any of the pairwise weekly comparisons (all $p > 0.05$).

Table 5: Pairwise Comparisons of Temporal Succession for the small size fraction (0.22-5 µm). Results of post-hoc pairwise comparisons between sampling weeks. The table displays estimated differences (Estimate), standard errors (SE), test statistics (*z* or *t* ratios), and adjusted *p*-values for each diversity index. Note: All *p*-values were adjusted using the Benjamini-Hochberg (BH) method. Estimates for the observed ASV richness are on the log scale. Significance levels: *** $p < 0.001$; ** $p < 0.01$; * $p < 0.05$; ns: not significant ($p > 0.05$).

Comparison	Index	Estimate	SE	Test Statistics	*p* (adj.)
W1 – W2	Observed	-0.204	0.065	z = −3.14	**0.003****
	Shannon	-0.471	0.109	t = −4.31	**< 0.001*****
	Inv. Simp.	-2.790	2.330	t = −1.20	0.281 (ns)
W1 – W3	Observed	-0.304	0.065	z = −4.67	**< 0.001*****
	Shannon	-0.806	0.109	t = −7.38	**< 0.001*****
	Inv. Simp.	-10.384	2.330	t = −4.46	**< 0.001*****
W1 – W4	Observed	-0.328	0.065	z = −5.03	**< 0.001*****
	Shannon	-0.889	0.109	t = −8.14	**< 0.001*****
	Inv. Simp.	-11.896	2.330	t = −5.11	**< 0.001*****
W2 – W3	Observed	-0.099	0.066	z = −1.51	0.158 (ns)
	Shannon	-0.336	0.111	t = −3.02	**0.004****
	Inv. Simp.	-7.595	2.370	t = −3.21	**0.003****
W2 – W4	Observed	-0.123	0.066	z = −1.86	0.094 (ns)
	Shannon	-0.418	0.111	t = −3.77	**< 0.001*****
	Inv. Simp.	-9.106	2.370	t = −3.84	**< 0.001*****
W3 – W4	Observed	-0.024	0.066	z = −0.36	0.717 (ns)
	Shannon	-0.083	0.111	t = −0.74	0.459 (ns)
	Inv. Simp.	-1.511	2.370	t = −0.64	0.525 (ns)

3.3 Beta Diversity

3.3.1 Global Community Structure and Fraction Separation

The NMDS plot (Figure 3) illustrated a clear differentiation of microbial communities based on the two size fractions. The ordination, based on Bray-Curtis dissimilarities, showed a low stress value (0.083), indicating a highly reliable representation of the community distances. Two distinct clusters were visible, separating the ≥5 µm (blue) and 0.22-5 µm (orange) fractions.

Statistical analysis using PERMANOVA confirmed that size fraction was the dominant factor for explaining the variability in microbial community structure (Table 6). With an R^2 value of 0.483, the size fraction factor explained approximately 48.3% of the total variance, showing highly significant differences between the two fractions ($F = 142.42$; $p < 0.001$).

The sampling week also had a highly significant influence ($p = 0.001$), accounting for 10.0% of the variance ($R^2 = 0.100$). Furthermore, a significant interaction between the week and the size fraction was observed ($R^2 = 0.057$; $F = 5.61$; $p < 0.001$), suggesting that the temporal succession followed slightly different patterns within the two fractions. Overall, the

investigated factors examined explained 64.0% of the total observed variance in community structure.

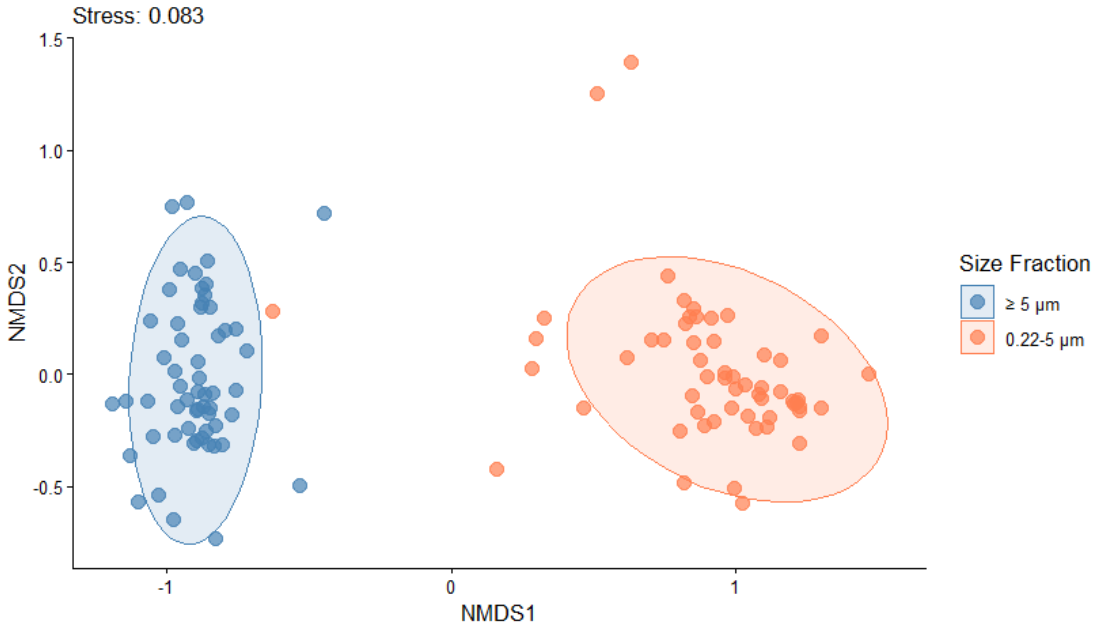

Figure 3: Microbial community structure across different size fractions. Non-metric multidimensional scaling (NMDS) ordination based on Bray-Curtis dissimilarities of relative ASV abundances. Points represent individual samples, colored by size fraction (≥5 µm, blue; 0.22-5 µm, orange). Ellipses indicate the 95% confidence interval for each group. NMDS stress = 0.083.

In contrast, the factor station explained a negligible and non-significant proportion of variance in community structure ($R^2 = 0.004$, $F_{1,112} = 0.503$, $p = 0.695$), indicating no meaningful spatial differentiation between sampling locations across the study period, which is further supported by the extensive overlap of station clusters in the global NMDS ordination (Figure S 8).

Table 6: Results of the permutation multivariate analysis of variance (PERMANOVA) on community structure. The influence of the factors sampling week (treated as a categorial factor), size fraction, and their interaction on the composition of microbial communities was investigated. The analysis is based on Bray-Curtis distances (relative abundance standardized) with 999 permutations, restricted within stations (blocks) to account for spatial autocorrelation. The degrees of freedom (*df*), sums of squares, explanatory power (R^2), *F*-statistic, and p-value are given. Significance levels: *** $p < 0.001$; ** $p < 0.01$; * $p < 0.05$.

Source of Variation	*df*	Sum of Squares	R^2	*F*	*p*
Sampling Week	3	2.89	0.100	9.77	**< 0.001** ***
Size Fraction	1	14.02	0.483	142.42	**< 0.001** ***
Week : Fraction	3	1.66	0.057	5.61	**< 0.001** ***
Residuals	106	10.44	0.360		
Total	113	29.00	1.000		

Analysis of the multivariate homogeneity of group dispersions (BETADISPER; Table 7) confirmed that the variances were homogeneously distributed across the main factors. No

significant differences in dispersion were found between the two size fractions ($F_{1,112} = 0.184$; $p = 0.670$) or between sampling weeks ($F_{3,110} = 0.863$; $p = 0.432$). These results met the statistical requirements for PERMANOVA and ensured that the different clusters observed in the NMDS ordination (Figure 3) were based on actual differences in community composition and not on artifacts of unequal group variances.

Table 7: Analysis of the multivariate homogeneity of group dispersions (BETADISPER). Analysis of the variance (dispersion) within the factors sampling week (treated as a categorical factor) and size fraction. The calculation is based on Bray-Curtis distances (relative abundance standardized) with 999 permutations. Permutations were restricted within water samples (for size fraction) and stations (for sampling week) to account for the repeated measures design and the paired nature of the filter fractions. The degrees of freedom (*df*), sums of squares, mean squares, *F*-statistics, and *p*-values (*Pr*(>*F*)) are specified.

Factor	*df*	Sum of Squares	Mean Square	*F*	*p* (*Pr*(>*F*))
Sampling Week	3	0.0120	0.0040	0.863	0.432
Residuals	110	0.5111	0.0046		
Size Fraction	1	0.0022	0.0022	0.184	0.670
Residuals	112	0.3603	0.0121		

3.3.2 Temporal Succession Within Size Fractions

Within each size fraction, sampling week had a significant effect on community composition. PERMANOVA revealed a highly significant effect of sampling week on community composition in both fractions, explaining 24.1% of the variation in the large fraction ($R^2 = 0.241$, $F_{1,55} = 17.46$, $p = 0.001$) and 21.6% in the small fraction ($R^2 = 0.216$, $F_{1,55} = 15.20$, $p = 0.001$). ANOSIM supported these results, indicating a moderately strong temporal signal ($R = 0.420$ and $R = 0.359$, respectively, $p = 0.001$ in each case). Since multivariate dispersion was not significant in either fraction (betadisper, $p = 0.869$ and $p = 0.138$, respectively), these differences can be interpreted as robust compositional changes over the study period rather than artefacts of unequal within-group variation.

3.3.3 Temporal Community Turnover

To quantify the rate of temporal change over the study period, two measures were calculated: the abundance-based Bray-Curtis dissimilarity and the presence/absence-based Jaccard dissimilarity between consecutive weeks, used as a measure of temporal turnover (Figure 4).

The following mean values (mean ± SE, averaged across all stations) were obtained for the Bray-Curtis dissimilarities: between week 1 and week 2, the dissimilarity was 0.329 (± 0.025 SE) for the large fraction (≥5 µm) and 0.300 (± 0.024 SE) for the small fraction (0.22–5 µm). In the interval from week 2 to week 3, the dissimilarities were similar between fractions; the

small fraction showed values of 0.405 (± 0.025 SE) and the large fraction 0.370 (± 0.042 SE). The highest Bray-Curtis values were observed between week 3 and week 4: 0.430 (± 0.045 SE) in the small fraction and 0.423 (± 0.030 SE) in the large fraction.

The temporal turnover based on presence/absence, measured as the mean Jaccard dissimilarity between consecutive weeks (averaged across all stations), showed values in the range of approximately 0.56 to 0.62 in both size fractions. Between week 1 and week 2, the mean turnover was 0.586 (± 0.017 SE) for the small fraction and 0.560 (± 0.019 SE) for the large fraction. In the interval from week 2 to week 3, the values were 0.599 (± 0.016 SE) in the small fraction and 0.587 (± 0.020 SE) in the large fraction. Between week 3 and week 4, values of 0.615 (± 0.016 SE) were observed for the small fraction and 0.571 (± 0.013 SE) for the large fraction.

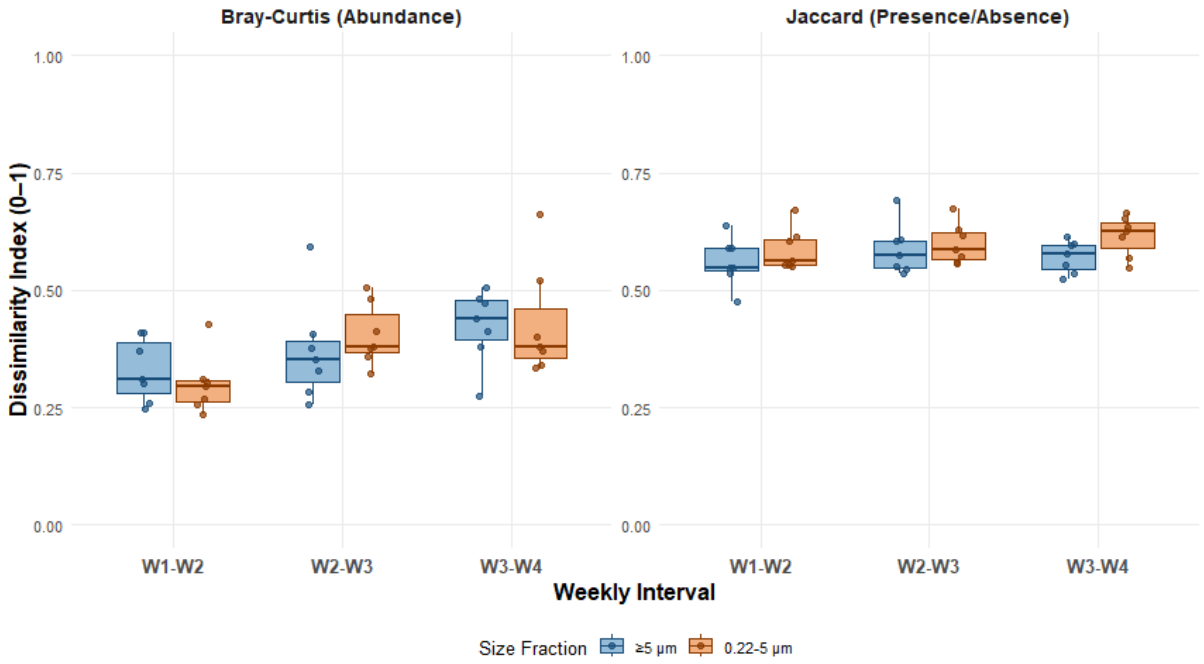

Figure 4: Weekly community dynamics of size fractions. Box plots illustrate the distribution of Bray-Curtis dissimilarities (left) and Jaccard turnover (right) between consecutive weeks. Lines within boxes indicate the median; boxes represent the interquartile range (IQR). Individual points represent the dissimilarity values of individual sampling stations, calculated from weekly mean relative abundance profiles. Colors indicate the large (≥5 µm, blue) and small (0.22–5 µm, orange) size fractions.

3.4 Drivers of Community Successional Dynamics

In the large fraction, nitrite correlated significantly with the community structure in the envfit analysis (Table 8); dissolved oxygen (r^2 = 0.121, p = 0.087) and chlorophyll *a* showed a statistical trend. In PERMANOVA (Table S 6), nitrite (R^2 = 0.044, F = 2.417, $Pr(>F)$ = 0.033)

was a significant influencing factor; ammonium showed a trend ($R^2 = 0.039$, $F = 2.148$, $Pr(>F) = 0.061$).

In the small fraction, the envfit analysis (Table 8) revealed significant correlations for dissolved oxygen and nitrite ($r^2 = 0.166$, $p = 0.050$); chlorophyll *a* and salinity showed a trend. PERMANOVA identified dissolved oxygen ($R^2 = 0.063$, $F = 3.624$, $Pr(>F) = 0.004$) as a significant marginal driver.

The key findings in brief: nitrite was significant in the large fraction in both envfit and PERMANOVA, and in the small fraction in envfit; dissolved oxygen was significant in the small fraction in both analyses, while showing only a trend in the large fraction (envfit $p = 0.087$). Ammonium showed a trend in the large fraction in PERMANOVA only, as did salinity in the small fraction in envfit only.

Table 8: Results of the environmental vector fitting analysis (envfit). The table shows the coefficients of determination (r^2) and empirical p-values ($Pr(>r)$) for the correlation of abiotic variables with the microbial community structure. The analysis is based on NMDS ordinations (Bray-Curtis distances of relative abundance data) and was performed separately for the large (≥5 µm) and small (0.22-5 µm) fractions. To account for the sampling design, permutations (n = 999) were blocked within stations. Significance levels: * $p < 0.05$; . $p < 0.1$ (trend); ns: not significant ($p > 0.05$).

Environmental Parameter	Fraction	r^2	$Pr(>r)$
Nitrite	≥5 µm	0.182	**0.025 ***
	0.22-5 µm	0.166	**0.050 ***
Dissolved Oxygen	≥5 µm	0.121	0.087 .
	0.22-5 µm	0.206	**0.016 ***
Silicate	≥5 µm	0.059	0.144 (ns)
	0.22-5 µm	0.033	0.289 (ns)
Chlorophyll *a*	≥5 µm	0.067	0.082 .
	0.22-5 µm	0.077	0.066 .
Temperature	≥5 µm	0.034	0.585 (ns)
	0.22-5 µm	0.097	0.131 (ns)
Nitrate	≥5 µm	0.144	0.127 (ns)
	0.22-5 µm	0.125	0.243 (ns)
Ammonium	≥5 µm	0.136	0.199 (ns)
	0.22-5 µm	0.048	0.518 (ns)
Salinity	≥5 µm	0.011	0.768 (ns)
	0.22-5 µm	0.066	0.099 .
Phosphate	≥5 µm	0.005	0.921 (ns)
	0.22-5 µm	0.010	0.840 (ns)

The separate representation of the two size fractions using NMDS clearly showed a temporal shift in the microbial communities over the four-week study period (Figure 5). In the large fraction, the confidence ellipses for weeks 1 and 2 still showed a clear overlap, while week 3 overlapped with all other weeks and week 4 was more clearly separated from the earlier periods. In the small fraction (0.22–5 µm), a directed temporal sequence of the weekly clusters was also

apparent, with the samples from week 4 showing a comparatively wide spread and all ellipses overlapping (though only slightly in some cases).

In both fractions, the nitrite vector aligned with the ordination region predominantly occupied by few week 4 samples, while most week 4 samples were scattered across the upper ordination space, suggesting only a partial association between nitrite concentration and community composition in the later sampling period. In the small fraction, a few week 3 samples were additionally located in proximity to the nitrite vector, indicating that this association was not exclusively confined to the later sampling period. In contrast, the dissolved oxygen vector in the small fraction pointed towards the ordination region occupied by the early sampling weeks (weeks 1 and 2), suggesting an association between higher dissolved oxygen concentrations and community composition in the earlier sampling period.

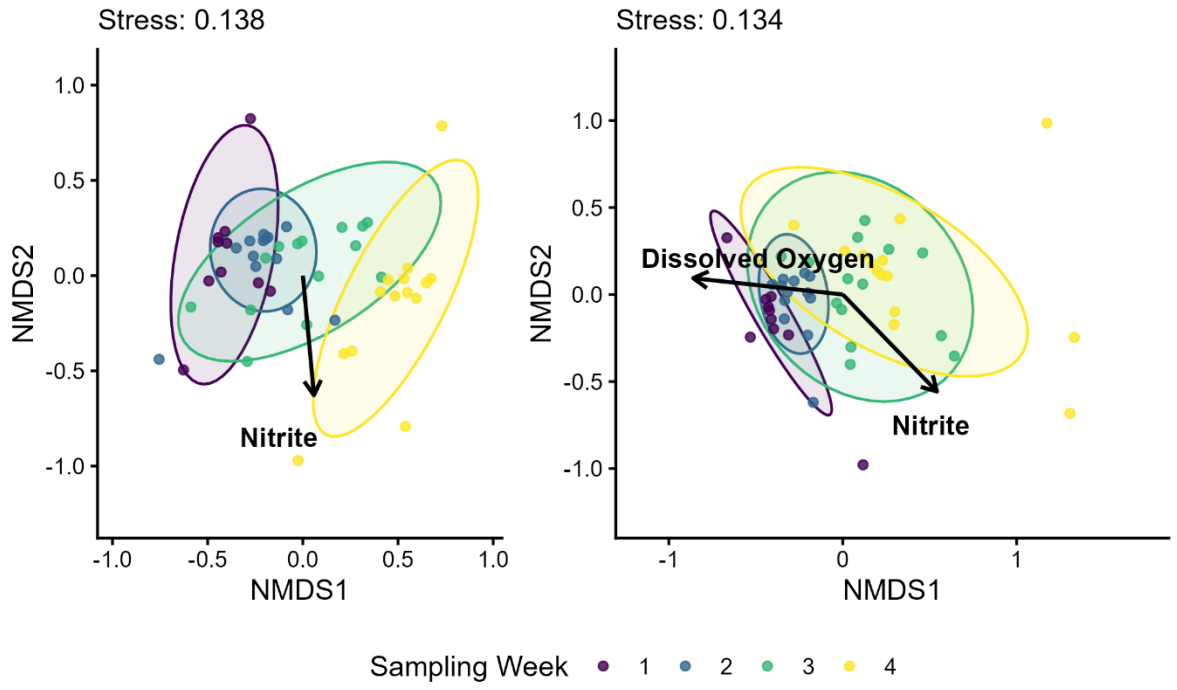

Figure 5: Non-metric multidimensional scaling (NMDS) ordination of microbial communities with projected environmental parameters (vector fitting; envfit). The analysis was performed separately for the large fraction (≥5 µm, left) and the small fraction (0.22-5 µm, right) based on Bray-Curtis dissimilarities following relative abundance transformation. The data points are color-coded according to the four sampling weeks in July, with the ellipses representing 95% confidence intervals of the weekly clusters. Black vectors represent significant correlations ($p < 0.05$) with abiotic factors; the length of the arrow corresponds to the strength of the correlation (r^2), while the direction indicates the gradient of the strongest increase in the respective parameter. The stress values (0.138 and 0.134) provide a reliable two-dimensional representation of community dynamics.

3.5 Microbial Eukaryotic Community Composition

The analysis of the taxonomic community composition at the class level (or highest taxonomic resolution available) highlighted the structural differences between the two size fractions during the study period (Figure 6). The large fraction showed high temporal stability across all stations (stations 3 and 19 showed slight variance) and was dominated by reads from groups such as Trebouxiophyceae, Syndiniales, Mediophyceae, and Dinophyceae. In contrast, the small fraction showed a significantly more dynamic development, characterized by high relative read abundances of groups such as Mamelliophyceae, Perkinsida, Chrysophyceae, and Pedinophyceae, as well as pronounced temporal fluctuations.

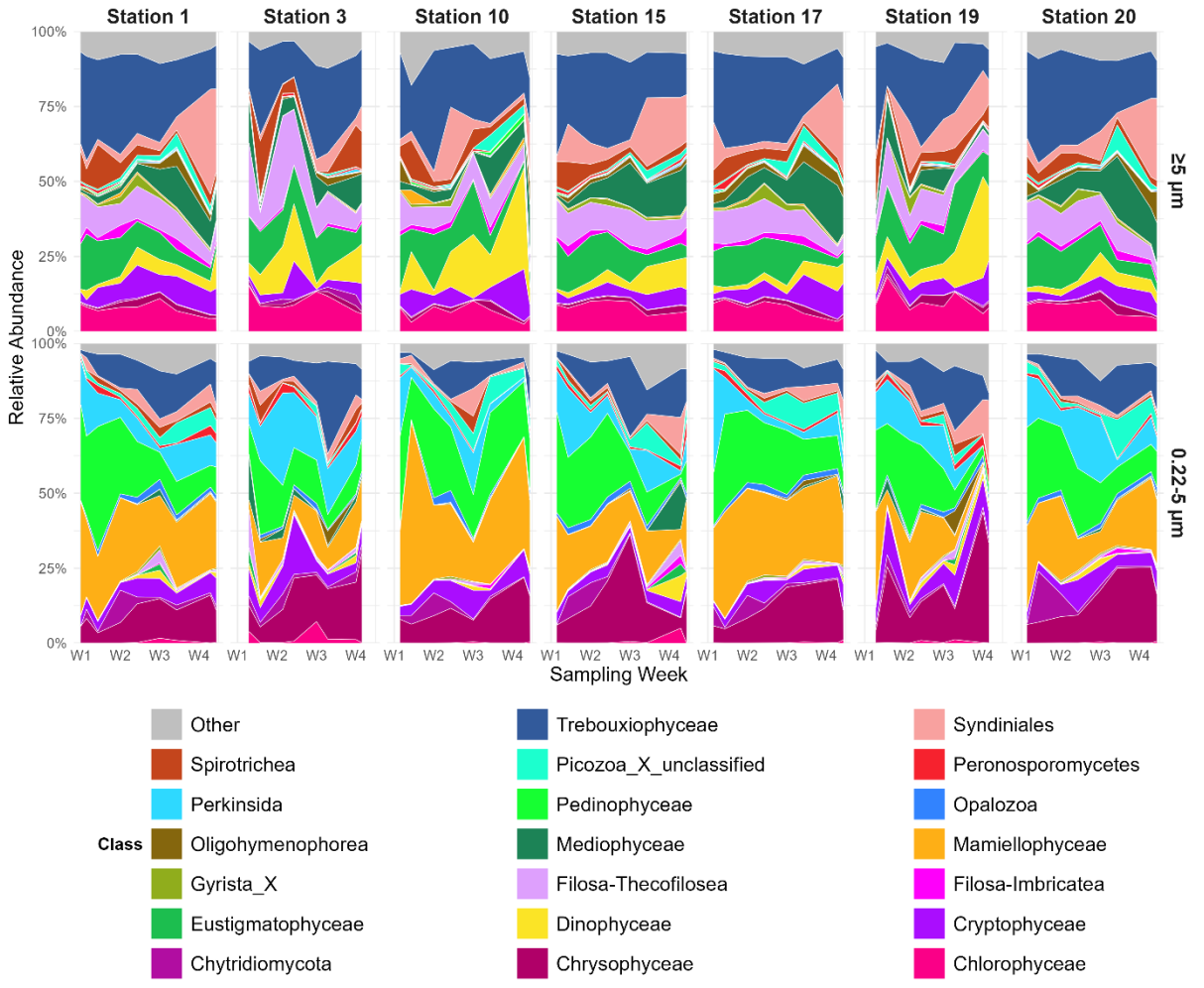

Figure 6: Top 20 taxonomic groups (class level). The figure shows the relative read abundance of the 20 most common classes at seven sampling stations (stations 1, 3, 10, 15, 17, 19, and 20) during the study period in July 2025. Taxonomic labels reflect PR2 database annotations at the class rank. The upper panels show the large fraction (≥5 µm), the lower panels show the small fraction (0.22–5 µm). Colors indicate different taxonomic classes; 'Other' summarizes all remaining taxa. The x-axis reflects actual sampling dates labeled by sampling week (W1–W4).

A clear temporal succession was observed, particularly in the small fraction: while reads from Mamelliophyceae increased in the middle of the month (weeks 2 and 3) at stations such as 10 and 20, Perkinsida and Trebouxiophyceae decreased in relative read abundance, especially at stations 1, 15, 17, 19, and 20. Occasional peaks, such as the increase in the relative abundance of Chrysophyceae reads at stations 15 and 19 in weeks 3 and 4, underscored the variability of this fraction. Although Syndiniales was represented in both size fractions, it accounted for a more prominent proportion of reads in the large fraction at almost all sites. Despite these temporal shifts, the basic taxonomic pattern remained largely consistent spatially across all seven stations within the respective fraction.

The taxonomic composition at the genus level (or highest taxonomic resolution available; Figure 7) confirms the trends already observed in Figure 6, and reveals specific succession patterns within the size fractions. In the large fraction, genera such as *Picochlorum*, *Cyclotella*, and *Monodus* represented the largest fraction of reads throughout the study period. In addition, an increase in the relative read abundance of the Syndiniales lineage (*Dino-Group-I-Clade-4_X)* was observed at almost all stations from week 1 to week 4. Compared to the smaller fraction, the proportion of 'Other' remained considerably higher and relatively constant in the large fraction.

The small fraction was characterized by more complex succession dynamics, with *Marsupiomonas* and *Ostreococcus* dominating in relative abundance at the beginning of July (Figure 7; W1-2). The taxonomic structure remained relatively stable at most stations, consisting of dominant groups such as members of the Perkinsida, *Picochlorum*, Picozoa lineages, Paraphysomonadales (Clade-EC1Ga_X), and *Falcomonas*.

In general, the trend at all stations shows that the majority of the top 20 dominant genera decreased in relative read abundance over the course of the month. Station 19 in particular saw a sharp decline in almost all dominant genera in favor of the 'Other' category.

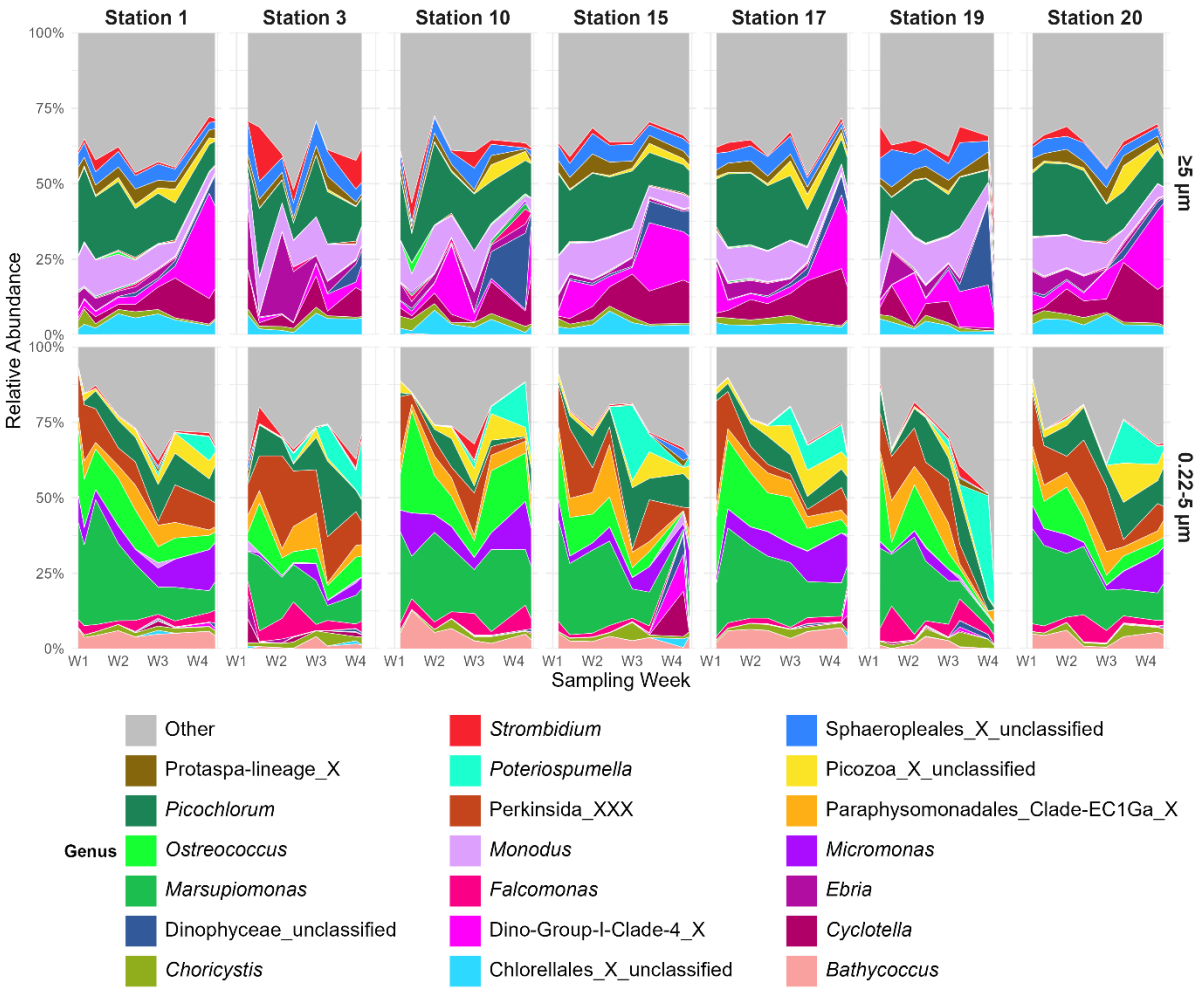

Figure 7: Top 20 taxonomic groups (genus level). The figure shows the relative read abundance of the 20 most common genera at seven sampling stations (stations 1, 3, 10, 15, 17, 19, and 20) during the study period in July 2025. Taxonomic labels reflect PR2 database annotations at the genus rank. The upper panels show the large fraction (≥5 µm), the lower panels show the small fraction (0.22–5 µm). Colors indicate different genera; 'Other' summarizes all remaining taxa. The x-axis reflects actual sampling dates labeled by sampling week (W1–W4).

4. Discussion

4.1 Size Fractionation showed distinct Microbial Eukaryotic Communities

The results of this study show that the size was an important factor in shaping the microbial eukaryotic community, as it was reflected in both alpha and beta diversity analyses. The large fraction showed higher mean alpha diversity and appeared relatively stable over the study period, while the small fraction had more pronounced temporal changes in diversity. These patterns suggest that the two size fractions represent ecologically distinct communities, differing in overall diversity levels and temporal stability. Their contrasting taxonomic compositions are discussed in Chapter 4.3. The consistently higher alpha diversity in the large fraction may reflect a broader range of trophic strategies available to larger-celled organisms, enabling greater niche differentiation (Barton et al., 2013; Wu & Liu, 2022). These findings are consistent with other studies that have found community composition to differ consistently between size fractions (De Vargas et al., 2015; Elferink et al., 2017; Massana et al., 2015; Wu & Liu, 2022). However, Wu & Liu (2022) and Elferink et al. (2017) reported higher alpha diversity in the picoeukaryote fraction, with diversity decreasing progressively toward larger cell sizes, a pattern that contrasts with the results of the present study (Elferink et al., 2017; Wu & Liu, 2022). Notably, both studies sampled coastal environments during summer, comparable in seasonality to the present study. Despite this, the diverging alpha diversity patterns suggest that geographic region and local environmental conditions may play a role in shaping diversity relationships between size fractions, with microbial eukaryote communities potentially responding differently across spatial scales even under similar seasonal conditions.

A methodological difference in size fractionation likely contributes to this discrepancy as well. Wu & Liu (2022) and Elferink et al. (2017) defined the picoeukaryote fraction as 0.22–3 µm and applied an upper boundary to their nanoeukaryote fraction (20 µm), whereas the present study used 0.22–5 µm for the smaller fraction and ≥5 µm with no defined upper limit for the larger fraction. The larger fraction in this study therefore encompasses both nano- and microeukaryotes, capturing a considerably broader size range than the narrowly defined nanoplankton fraction used in the other studies. This likely increases taxonomic richness within the larger fraction and may explain the higher alpha diversity observed in the ≥5 µm fraction compared to the more narrowly defined fractions in other studies. Similarly, De Vargas et al. (2015) analysed globally collected Tara Oceans samples spanning multiple ocean regions and seasons and reported higher alpha diversity in the pico-nano fraction (0.8–5 µm). This pattern that, while consistent at the global scale across diverse ocean regions and seasons, need not

apply uniformly at the local level, where site-specific environmental conditions and short-term dynamics may shift diversity relationships between size fractions. In light of this, the results of the present study may reflect the latter stages of a picoeukaryote bloom, suggested by the declining relative read abundances of initially dominant taxa including Mamiellophyceae, Pedinophyceae, and Perkinsida over the course of July. As this dominance weakened during the study period, abundances were redistributed, leading to the observed convergence of Shannon and Inverse Simpson values through increased evenness rather than a gain in species richness.

The higher alpha diversity in the larger fraction may further reflect differences in niche complexity between size classes. Although a weak but statistically significant positive correlation between sequencing depth and observed ASV richness was detected, sequencing depth did not differ significantly between size fractions, suggesting that the higher observed richness in the ≥5 µm fraction reflects genuine biological diversity rather than a sequencing artefact. Larger protists generally benefit more from elevated nutrient availability, as turbulence enhances nutrient flux disproportionately toward larger cells (Barton et al., 2014; Irwin et al., 2006; Karp-Boss et al., 1996). Smaller cells, by contrast, are more strongly governed by diffusion limitation and physical factors, which may reduce niche differentiation within the picoeukaryote community (Barton et al., 2014; Karp-Boss et al., 1996). More generally, cell size appears to modulate the sensitivity of microbial eukaryote communities to different environmental drivers, with smaller cells being more strongly governed by physical parameters such as temperature and salinity (Wu & Liu, 2022). Beyond nutrient dynamics, morphological diversity in protists appears to peak at intermediate cell sizes broadly overlapping with the ≥5 µm fraction, where cells show the greatest variety of shapes and may therefore occupy a wider range of ecological niches than the more uniformly spherical cells at size extremes (Hillebrand et al., 2022; Ryabov et al., 2021). Trophic flexibility, particularly mixotrophy, may further broaden niche space by decoupling growth from strict nutrient dependence (Barton et al., 2013).

In this context, the two fractions are best understood as operational size classes rather than strict equivalents of the classical plankton size categories. The ≥5 µm fraction may include not only nanoplankton in the strict sense, but also larger cells; moreover, partial taxonomic overlap between fractions, as reported by Massana et al. (2015) and Elferink et al. (2017), suggests that size-class boundaries are not absolute biological barriers, a pattern that cannot be excluded in the present dataset either. This methodological consideration is further supported by Haider et al. (2026), who found that size fractionation provides better resolution of microbial communities than unfractionated approaches, particularly during dynamic periods such as

seasonal blooms. While abundant taxa were largely shared between fractions, differences emerged primarily among rarer ASVs that would otherwise remain obscured in bulk samples, and size fractionation allowed for a distinction between free-living and particle-associated community members, yielding more ecologically meaningful insights into processes such as microbial succession and nutrient cycling.

4.2 Temporal Succession of the Community Structure in July

The temporal development of the community revealed pronounced dynamics within the four-week study period, with both fractions undergoing compositional change but at different rates. When assessed separately for each fraction, ANOSIM *R* values of 0.42 (large) and 0.36 (small), together with significant *p*-values of ANOSIM and PERMNOVA, indicated a moderate yet clear separation between sampling weeks, consistent with substantial restructuring on short time scales (K. R. Clarke, 1993). For such a short study interval, this suggests a relatively rapid temporal reassembly of the community. Similar short-term dynamics have been reported for marine protist communities during the transition from spring to summer, where pronounced shifts in composition occurred within days to weeks (Berdjeb et al., 2018), as well as in small eukaryotes in freshwater and coastal systems followed at high temporal resolution (Mangot et al., 2013; Nagarkar et al., 2018).

These temporal changes were accompanied by contrasting alpha diversity trajectories in the two size fractions. The large fraction showed no significant pairwise differences between weeks for any alpha diversity index, while the small fraction increased continuously from week 1 to week 3 before stabilizing in week 4. This contrasting trajectory suggests that the two fractions responded differently to the environmental conditions prevailing during July, with the small fraction undergoing more pronounced short-term restructuring. However, sequencing depth varied significantly across sampling weeks (Kruskal-Wallis, $X^2 = 12.23$, $df = 3$, $p = 0.007$), which may partially confound temporal comparisons of observed ASV richness and should be considered a limitation of this study.

The tendency of the small fraction to show stronger short-term variability is consistent with the known capacity of picoeukaryotes to respond rapidly to environmental fluctuations. Their short generation times and high potential growth rates allow these organisms to track changes in environmental conditions on time scales of days, resulting in marked diversity fluctuations over short intervals (Jacquet et al., 2001; Mangot et al., 2013; Vaulot & Marie, 1999). The overall

increase in alpha diversity across the sampling period, with values appearing to plateau in week 4, combined with the slight decline in evenness in the larger fraction over the same period, may be consistent with a transitional phase following an earlier restructuring event or bloom-like development, though the four-week sampling window does not allow definitive conclusions about whether this pattern represents stabilisation or a temporary plateau. Comparable patterns with rapid shifts in richness and community composition and many OTUs occurring only transiently over weekly time scales, have been reported from coastal Pacific eukaryotic microbial communities (Nagarkar et al., 2018).

Additional insight into the rate and nature of compositional change was provided by Bray–Curtis dissimilarity and Jaccard turnover. Bray–Curtis dissimilarities between consecutive weeks ranged around 0.36–0.47 in both fractions, indicating a moderate degree of compositional change from week to week without evidence for a strong acceleration over the month. Jaccard dissimilarities were high (between 0.54 and 0.62), that indicates that less than half of the taxa were shared between successive weeks, which may point to substantial compositional turnover rather than merely shifts in relative abundance. Similar levels of short-term reassembly have been reported for small eukaryotic communities in other systems, where high dissimilarity between consecutive sampling dates reflects ongoing succession on weekly time scales (Mangot et al., 2013). A predominance of turnover over richness differences has likewise been reported for Baltic Sea phytoplankton communities, where 64–65% of beta diversity was attributed to species turnover and only 35–36% to richness differences (Olli et al., 2023).

Most notably, both size fractions showed comparable levels of temporal turnover between consecutive weeks, displaying similarly high dissimilarities despite their contrasting alpha diversity dynamics. The parallel magnitude of change in both fractions suggests that a shared environmental process drove community-wide restructuring, even if the specific mechanisms and rates differed between them. Protist time-series from the Skagerrak have likewise revealed strong temporal variation, with seasonal shifts affecting multiple major taxonomic groups and temperature emerging as a dominant abiotic driver of community change (Gran-Stadniczenko et al., 2018). The two size fractions should therefore not be viewed as fully independent compartments: trophic coupling between fractions (for example through grazing, parasitism, or mixotrophy) may have amplified the observed dynamics. Mangot et al. (2013) similarly emphasized that the dynamics of small eukaryotic diversity cannot be understood in isolation from other planktonic components and that assembly processes may differ among functional

groups. Overall, the observed patterns are more consistent with an intensified short-term succession than with simple destabilization of the community.

4.3 Taxonomic Composition and Functional Interpretation

This exploratory overview of the microbial eukaryote community revealed that both fractions were highly diverse, encompassing a range of different lifestyles and trophic strategies. Focusing on the autotrophic community, clear differences between the fractions became apparent. While larger-celled or colonial groups like Chlorophyceae and Mediophyceae (diatoms) were prominent in the large fraction, the small fraction was distinctly dominated by pico-sized green algae, particularly Mamiellophyceae.

Mixotrophic groups such as Cryptophyceae, Chrysophyceae and Dinophyceae were present in both fractions, highlighting the widespread occurrence of mixotrophy across phylogenetically distinct lineages (S. R. Anderson & Harvey, 2020; Mangot et al., 2009). At the same time, important heterotrophic consumers such as ciliates (Oligohymenophorea and Spirotrichea), Filosea (Imbricatea, Thecofilosea), and heterotrophic stramenopiles (Opalozoa and Gyrista), as well as unclassified Picozoa, were detected in both fractions, albeit at comparatively low relative read abundances.

In the large fraction, the dominant groups such as Trebouxiophyceae, Mediophyceae, and Dinophyceae remained relative stable throughout the sampling period. This consistency, along with the steady proportion of less abundant taxa (grouped as ‘Others’), reflects the structural buffering that was already suggested by the alpha diversity analysis. In contrast, the small fraction showed more distinct shifts among its dominant groups, including Mamiellophyceae, Perkinsida, Chrysophyceae, and Pedinophyceae. This higher temporal variability and the increasing share of the ‘Others’ group in the picoplankton highlight that this fraction was more dynamic over time.

The largest relative read abundance in the large fraction was contributed by Trebouxiophyceae, a group dominated by *Picochlorum* but also including *Choricystis* and Chlorellales_X_unclassified. Members of this class, including *Picochlorum* and *Chlorella*, are commonly found in coastal and nearshore waters (Fucikova et al., 2014; Tragin et al., 2016), while *Choricystis* has been found in freshwater or brackish environments (Kulakova et al., 2020). Their high relative abundance in the Greifswalder Bodden may therefore be linked to a broad tolerance to environmental variability, particularly salinity fluctuations. In this context,

Foflonker et al. (2016) described a *Picochlorum* strain isolated from a brackish lagoon that exhibited pronounced euryhalinity, suggesting that this genus is well adapted to the fluctuating conditions characteristic of estuarine and lagoonal systems. It is likely that additional Trebouxiophyceae taxa were present but fell below the threshold of the 20 most abundant groups, indicating that their overall contribution may be even broader than captured here.

Parasitic protist groups formed a substantial component of the community. Syndiniales, marine alveolate protist parasites, were present in both fractions and were particularly abundant in the large fraction, especially *Dino-Group-I-Clade-4_X*, which is commonly associated with parasitic interactions in marine protist communities (Q. Xu et al., 2021). Similar observations were reported by Haider et al. (2026) and Froján et al. (2025), while data from the Tara Oceans expedition demonstrated that Syndiniales represent a globally important component of microbial eukaryote communities, often with high relative abundances in the picoplankton fraction (De Vargas et al., 2015). Although Syndiniales were also detected in the small fraction in the present study, their comparatively high read abundance in the large fraction suggests a close association with larger host organisms such as dinoflagellates and diatoms, which are also predominantly found in this fraction (S. R. Anderson & Harvey, 2020; Sehein et al., 2022).

Both Anderson & Harvey (2020) and Sehein et al. (2022) reported pronounced temporal variability in Syndiniales, with peak abundances during summer months. As the present study covers only a limited time period, it remains unclear whether similar seasonal patterns occur in the GWB. In addition to Syndiniales, the presence of Perkinsida, particularly in the small fraction, further points towards the importance of parasitic or host-associated processes. Members of this group, which belong to the Alveolata, have been reported mainly from freshwater systems but have also been detected in marine environments in recent years (Lefranc et al., 2005; Ortiz-Álvarez et al., 2018). Together with Chytridiomycota, these parasitic lineages highlight the importance of biotic interactions in structuring microbial eukaryote communities, even though sequence-based data do not allow direct conclusions about their ecological activity.

Within the picoplankton, Mamiellophyceae showed the highest relative abundances. The associated genera *Bathycoccus*, *Micromonas* and *Ostreococcus* are among the most dominant picoeukaryotes worldwide (Grimsley et al., 2015; Massana et al., 2015; Tragin & Vaulot, 2019). While one study reported phagotrophic capabilities in a *Micromonas* strain (McKie-Krisberg & Sanders, 2014), this observation was not confirmed under experimental conditions by (Jimenez & Burns, 2021), indicating that the extent of mixotrophy in green algae remains unresolved. Although Mamiellophyceae were mainly confined to the small fraction in the present study, a

small proportion was also detected in the large fraction. Similar patterns have been reported previously, with potential filtration artefacts discussed as one explanation when interpreting size-fractionated molecular data (Massana et al., 2015). In addition to the Mamiellophyceae, the Pedinophyceae, a group of small green algae represented by Marsupiomonas (Turmel et al., 2020), were also abundant in the small fraction, highlighting the contribution of autotrophic taxa to the picoplankton community.

The taxonomic composition provides a more detailed picture of the ecological processes underlying the observed patterns. The Tara Oceans survey confirmed that eukaryotic plankton diversity is strongly structured across size fractions, with smaller fractions harboring distinct communities dominated by heterotrophic and parasitic protists (De Vargas et al., 2015). In contrast, the small fraction in the present study was predominantly characterized by autotrophic taxa such as Pedinophyceae, Mamiellophyceae, and Chrysophyceae. The co-occurrence of groups such as dinoflagellates, diatoms, and ciliates alongside parasites like Syndiniales and Perkinsida suggests a community primarily shaped by biotic interactions, such as predator-prey and parasite-host dynamics (cf. Massana et al., 2015). Notably, Anderson & Harvey (2020) found that environmental parameters explained very little of the variation in Syndiniales composition. This suggests that biological relationships are the more dominant driver, particularly as Syndiniales often act as parasitoid regulators that proliferate once host populations (e.g., diatoms or dinoflagellates) reach a peak. This aligns with the broader idea that interactions like grazing and parasitism can often exert a stronger influence on microbial eukaryote community structure than abiotic factors alone (Bock et al., 2020).

4.4 Environmental Drivers of Community Dynamics

Protists are surrounded by various types of stress, either biotic (e.g. parasitic interactions or predator–prey relationships) or abiotic (e.g. environmental factors such as temperature, salinity, radiation, and nutrients) (Slaveykova et al., 2016). Stress responses can be manifold and may, among other things, lead to a restructuring of the protist community (Albagly & Rahav, 2026; Slaveykova et al., 2016). The results of the present study suggest that the shifts in community structure observed in July were potentially associated with some abiotic factors. Subtle differences in the possible correlations or associations with abiotic stressors between the two size fractions may be explained by the fact that smaller cells possess a more favorable surface-to-volume ratio, enabling them to respond more rapidly to immediate chemical fluctuations than larger cells (Raven, 1998).

According to the significant PERMANOVA results, the nanoeukaryotic community was significantly influenced by nitrite, while ammonium showed a marginal trend. Additionally, envfit revealed that the nitrite vector was associated with samples from the later sampling period. Similar findings were reported by McQuatters-Gollop et al. (2024) in the Western English Channel. They demonstrated that plankton groups showed coherence with components of the nitrogen cycle. Nitrite displayed a negative correlation with heterotrophic nanoeukaryotes, which the authors attributed to heterotrophic decomposition of dissolved organic nitrogen compounds. Associations of pico- and nanoeukaryotes with components of the nitrogen cycle were similarly observed by Grattepanche et al. (2022). Heterotrophic protists and dinoflagellates play an important role in regenerating ammonium (Glibert, 1998) and may therefore be associated with elevated ammonium concentrations.

The small fraction community was significantly correlated with dissolved oxygen, while salinity showed a marginal trend in envfit. Since the nitrite vector did not point clearly towards a specific sampling period, it remains unclear whether a spatial component may also be involved, this would, however, require further investigation. Wang et al. (2019) found that the relative metabolic activity of picoeukaryotes, such as Mamiellophyceae, was substantially influenced by nutrient concentrations including nitrate, nitrite, and silicate, suggesting that similar taxa identified in the present study may have been affected in a comparable manner. Salinity has been identified as a strong driver of eukaryotic plankton community composition (Grattepanche et al., 2022; Hu et al., 2016; F. Wang et al., 2019), and the trend observed here may reflect a subtle but biologically relevant influence consistent with these findings. In contrast, dissolved oxygen showed an association with samples from Week 1, suggesting that dissolved oxygen availability was higher at the beginning of July and declined over the course of the month, potentially driven by heterotrophic respiration or decomposition processes (Del Giorgio, 2005).

However, Piwosz et al. (2018) found that a large proportion of the observed variability in pico- and nanoeukaryotic communities was explained by a combination of multiple environmental parameters, suggesting that future studies should consider that the effects of individual environmental factors may differ from those of interactions among several environmental factors. The impact of environmental factors on microbial communities can vary across different geographic scales. The study by De Vargas et al. (2015) demonstrated that communities within the same size fraction often share higher similarities across thousands of kilometers than different-sized communities at the same location. However, it is important to

note that their study primarily focused on open marine environments, whereas the GWB is a shallow, brackish system. While the present study found no significant differences in overall community structure between the sampling stations, this might be due to the relatively small geographic scale or the well-mixed nature of this coastal bay. A key limitation, however, was the short investigation period. Further research over longer timeframes is therefore recommended to determine whether seasonal trends lead to site-specific community variations across different locations within the GWB.

4.5 Limitations

Before discussing methodological causes of bias, some limitations of the study design should be noted. The study was based on an exploratory sampling design with seven different stations, no true replicates, and weather-dependent sampling, which limited both the spatial balance of the dataset and the temporal resolution of the observations. Due to weather-dependent sampling, samples could not be taken at regular intervals, which is why the time scales are shown in weeks (with two samples per week per station) rather than in sampling days. More regular sampling can provide a higher-resolution view. Therefore, the study was better suited to identify general short-term patterns in the dynamics of microbial eukaryotic communities than to make definitive conclusions about spatial structure or more precise succession. Future studies would benefit from a more even distribution of stations, especially between coastal and more open lagoon areas, as well as a more regular sampling schedule and the inclusion of replicates.

At the same time, the sequencing depth achieved in this study was sufficient to capture most of the microbial eukaryotic diversity present in July, suggesting that the dataset provides a solid basis for community-level analyses. Nevertheless, despite good sequence coverage, the ecological interpretation of metabarcoding data is subject to methodological limitations and potential biases that should be carefully considered. Varying copy numbers of the 18S amplicon can lead to misleading results. Alveolates are known to possess a higher number of gene copies (Prokopowich et al., 2003); it is therefore important not to assume absolute abundance, but rather to work with relative abundances and to exercise caution when drawing conclusions about biomass. A further source of bias in size-fractionated microbial samples may arise during filtration. Artefacts can occur due to broken larger cells passing into smaller size fractions, or due to smaller cells being retained on clogged filter pores. Both can influence the taxonomic composition and should be considered when interpreting the results (Massana et al., 2015). Furthermore, the use of Bray-Curtis dissimilarity on relative abundances emphasizes

differences among dominant taxa, while rare taxa contribute little to the calculated distances. Ecologically relevant but low-abundance groups may therefore be underrepresented in the beta diversity patterns reported here. Additionally, a minor fraction of reads (0.53% of total reads; *n* = 62,773 reads) was assigned to fungal taxa not typically associated with marine planktonic communities. As these taxa represent a negligible proportion of the dataset, they were retained in the analysis; their potential influence on community-level patterns is considered minimal.

5. Conclusion

Despite the artificially imposed boundary at 5 µm introduced by size fractionation, the microbial eukaryote communities of the Greifswalder Bodden showed clear differences between the two size fractions that likely reflect genuine biological patterns rather than methodological artefacts alone. The large fraction (nanoeukaryotes) was primarily associated with nitrogen cycling, whereas the small fraction (picoeukaryotes) appeared to be more strongly influenced by dissolved oxygen availability. However, there were no observations of environmental parameters such as temperature and salinity significantly shaping the microbial eukaryotic community over this short period of four weeks in the GWB.

The relative decline in read proportions of the most abundant genera within the picoeukaryote fraction reflects increasing evenness and suggests a transition from bloom-like dynamics towards a more balanced community. The large fraction, by contrast, remained comparatively stable throughout most of the sampling period, with signs of a more pronounced shift only towards the end. Overall, a restructuring of the entire community took place during the study period, as reflected by the relatively high turnover rates observed in both fractions.

Beyond the influence of environmental parameters, biotic interactions also appear to play an important role, as suggested by the taxonomic composition. Parasites in particular seem to be key players in this dynamic system, accounting for a substantial proportion of relative read abundances and occurring in both fractions. They may critically shape the course of algal blooms and drive community restructuring.

5.1 Outlook

The use of the two filter sizes in this study provided a deeper insight into the microbial eukaryotic community of the GWB. The potential of size fractionation could be further maximized by incorporating additional filter sizes and replicates to mitigate filter bias. Future research should consider integrating eDNA analysis with quantitative methods, such as qPCR or ddPCR, alongside microscopy. Such an approach would yield more robust data for examining community dynamics in terms of abundance and biomass, as well as the impacts of environmental and anthropogenic pressures such as nutrients or rising temperatures.

While the aim of this study was to provide an overview of short-term changes within the protist community, understanding long-term variations and potential seasonal patterns requires an extended investigation period. This study captures only a brief snapshot of the summer and is therefore limited in its ability to characterize broader temporal community shifts. When viewed within a wider temporal context, these results may be subject to different interpretations. Additionally, few significant correlations between community dynamics and environmental parameters were observed in this study. An extended investigation period may enable the detection of subtler relationships between protists and their environment.

Given that environmental drivers often vary spatially, expanding the study area to encompass the entire GWB, where logistically feasible, would be of great interest. This could include comparing nearshore stations with those in more open waters to specifically investigate the extent of terrestrial influence. While certain trends and shifts in community dynamics were visible in the taxonomic breakdowns of the stacked area charts, the composition also revealed that several taxa and groups could not yet be identified to the class or genus level. This underscores the ongoing need for further research to continue deciphering the vast complexity of the protist world.

References

Adl, S. M., Bass, D., Lane, C. E., Lukeš, J., Schoch, C. L., Smirnov, A., Agatha, S., Berney, C., Brown, M. W., Burki, F., Cárdenas, P., Čepička, I., Chistyakova, L., Del Campo, J., Dunthorn, M., Edvardsen, B., Eglit, Y., Guillou, L., Hampl, V., … Zhang, Q. (2019). Revisions to the Classification, Nomenclature, and Diversity of Eukaryotes. *Journal of Eukaryotic Microbiology*, *66*(1), 4–119. https://doi.org/10.1111/jeu.12691

Adl, S. M., Simpson, A. G. B., Farmer, M. A., Andersen, R. A., Anderson, O. R., Barta, J. R., Bowser, S. S., Brugerolle, G., Fensome, R. A., Fredericq, S., James, T. Y., Karpov, S., Kugrens, P., Krug, J., Lane, C. E., Lewis, L. A., Lodge, J., Lynn, D. H., Mann, D. G., … Taylor, M. F. J. R. (2005). The New Higher Level Classification of Eukaryotes with Emphasis on the Taxonomy of Protists. *The Journal of Eukaryotic Microbiology*, *52*(5), 399–451. https://doi.org/10.1111/j.1550-7408.2005.00053.x

Albagly, E., & Rahav, E. (2026). *Does size matter? Pico-phytoplankton cell size affects biomass distribution and nutrient limitation in the oligotrophic Eastern Mediterranean Sea*. https://doi.org/10.5194/egusphere-2026-934

Anderson, D. M., Glibert, P. M., & Burkholder, J. M. (2002). Harmful algal blooms and eutrophication: Nutrient sources, composition, and consequences. *Estuaries*, *25*(4), 704–726. https://doi.org/10.1007/BF02804901

Anderson, S. R., & Harvey, E. L. (2020). Temporal Variability and Ecological Interactions of Parasitic Marine Syndiniales in Coastal Protist Communities. *mSphere*, *5*(3), e00209-20. https://doi.org/10.1128/mSphere.00209-20

Andersson, A., Zhao, L., Brugel, S., Figueroa, D., & Huseby, S. (2023). Metabarcoding vs Microscopy: Comparison of Methods To Monitor Phytoplankton Communities. *ACS ES&T Water*, *3*(8), 2671–2680. https://doi.org/10.1021/acsestwater.3c00176

Bálint, M., Pfenninger, M., Grossart, H.-P., Taberlet, P., Vellend, M., Leibold, M. A., Englund, G., & Bowler, D. (2018). Environmental DNA Time Series in Ecology. *Trends in Ecology & Evolution*, *33*(12), 945–957. https://doi.org/10.1016/j.tree.2018.09.003

Barton, A. D., Finkel, Z. V., Ward, B. A., Johns, D. G., & Follows, M. J. (2013). On the roles of cell size and trophic strategy in North Atlantic diatom and dinoflagellate communities. *Limnology and Oceanography*, *58*(1), 254–266. https://doi.org/10.4319/lo.2013.58.1.0254

Barton, A. D., Ward, B. A., Williams, R. G., & Follows, M. J. (2014). The impact of fine-scale turbulence on phytoplankton community structure. *Limnology and Oceanography: Fluids and Environments*, 34–49. https://doi.org/10.1215/21573689-2651533

Bates, D., Maechler, M., Bolker [cre, B., aut, Walker, S., Christensen, R. H. B., Singmann, H., Dai, B., Scheipl, F., Grothendieck, G., Green, P., Fox, J., Bauer, A., simulate.formula), P. N. K. (shared copyright on, Tanaka, E., Jagan, M., Boylan, R. D., & Ly, A. (2015). *lme4: Linear Mixed-Effects Models using "Eigen" and S4* [Computer software]. https://doi.org/10.18637/jss.v067.i01

Bauer, R. K., Stepputtis, D., Gräwe, U., Zimmermann, C., & Hammer, C. (2013). Wind-induced variability in coastal larval retention areas: A case study on Western Baltic spring-spawning herring. *Fisheries Oceanography*, *22*(5), 388–399. https://doi.org/10.1111/fog.12029

Berdalet, E., Fleming, L. E., Gowen, R., Davidson, K., Hess, P., Backer, L. C., Moore, S. K., Hoagland, P., & Enevoldsen, H. (2016). Marine harmful algal blooms, human health and wellbeing: Challenges and opportunities in the 21st century. *Journal of the Marine Biological Association of the United Kingdom*, *96*(1), 61–91. https://doi.org/10.1017/S0025315415001733

Berdjeb, L., Parada, A., Needham, D. M., & Fuhrman, J. A. (2018). Short-term dynamics and interactions of marine protist communities during the spring–summer transition. *The ISME Journal*, *12*(8), 1907–1917. https://doi.org/10.1038/s41396-018-0097-x

Bi, R., Cao, Z., Ismar-Rebitz, S. M. H., Sommer, U., Zhang, H., Ding, Y., & Zhao, M. (2021). Responses of Marine Diatom-Dinoflagellate Competition to Multiple Environmental Drivers: Abundance, Elemental, and Biochemical Aspects. *Frontiers in Microbiology*, *12*, 731786. https://doi.org/10.3389/fmicb.2021.731786

Blais, M.-A., Matveev, A., Lovejoy, C., & Vincent, W. F. (2024). Size-dependent community patterns differ between microbial eukaryotes and bacteria in a permafrost lake–river–sea continuum. *Limnology and Oceanography*, (69), 667–680. https://doi.org/10.1002/lno.12511

Bock, C., Jensen, M., Forster, D., Marks, S., Nuy, J., Psenner, R., Beisser, D., & Boenigk, J. (2020). Factors shaping community patterns of protists and bacteria on a European scale. *Environmental Microbiology*, *22*(6), 2243–2260. https://doi.org/10.1111/1462-2920.14992

Brooks, M., E., Kristensen, K., Benthem, K., J. ,van, Magnusson, A., Berg, C., W., Nielsen, A., Skaug, H., J., Mächler, M., & Bolker, B., M. (2017). glmmTMB Balances Speed and Flexibility Among Packages for Zero-inflated Generalized Linear Mixed Modeling. *The R Journal*, *9*(2), 378. https://doi.org/10.32614/RJ-2017-066

Callahan, B. J., McMurdie, P. J., Rosen, M. J., Han, A. W., Johnson, A. J. A., & Holmes, S. P. (2016). DADA2: High-resolution sample inference from Illumina amplicon data. *Nature Methods*, *13*(7), 581–583. https://doi.org/10.1038/nmeth.3869

Calvin, K., Dasgupta, D., Krinner, G., Mukherji, A., Thorne, P. W., Trisos, C., Romero, J., Aldunce, P., Barrett, K., Blanco, G., Cheung, W. W. L., Connors, S., Denton, F., Diongue-Niang, A., Dodman, D., Garschagen, M., Geden, O., Hayward, B., Jones, C., … Péan, C. (with Lee, H.). (2023). *IPCC, 2023: Climate Change 2023: Synthesis Report. Contribution of Working Groups I, II and III to the Sixth Assessment Report of the Intergovernmental Panel on Climate Change [Core Writing Team, H. Lee and J. Romero (eds.)]. IPCC, Geneva, Switzerland.* (First). Intergovernmental Panel on Climate Change (IPCC). https://doi.org/10.59327/IPCC/AR6-9789291691647

Charette, M., & Smith, W. (2010). The Volume of Earth's Ocean. *Oceanography*, *23*(2), 112–114. https://doi.org/10.5670/oceanog.2010.51

Clarke, K. R. (1993). Non-parametric multivariate analyses of changes in community structure. *Australian Journal of Ecology*, *18*(1), 117–143. https://doi.org/10.1111/j.1442-9993.1993.tb00438.x

Clarke, L. J., & Deagle, B. E. (2020). Eukaryote plankton assemblages in the southern Kerguelen Axis region: Ecological drivers differ between size fractions. *Deep Sea Research Part II: Topical Studies in Oceanography*, *174*, S0967064518300833. https://doi.org/10.1016/j.dsr2.2018.12.003

Cloern, J. E. (1996). Phytoplankton Bloom Dynamics in Coastal Ecosystems: A Review with some general Lessons from sustained Investigation of San Francisco Bay, California. *Reviewsof Geophysic*, *34*, 127–168.

Cognetti, G., & Maltagliati, F. (2000). Biodiversity and Adaptive Mechanisms in Brackish Water Fauna. *Marine Pollution Bulletin*, *40*(1), 7–14. https://doi.org/10.1016/S0025-326X(99)00173-3

Corliss, J. O. (2002). *Biodiversity and Biocomplexity of the Protists and an Overview of Their Significant Roles in Maintenance of Our Biosphere*.

Corrales-Ugalde, M., Luo, J. Y., Petrik, C. M., Stcok, C. A., Dugenne, M., Stemmann, L., O'Brien, T. D., & Kiko, R. (2025). Assessment of Plankton Size Structure From CMIP6 Earth System Models With a Novel Pelagic Size Structure Database. *Global Biogeochemical Cycles*, *39*(12). https://doi.org/10.1029/2024GB008443

Davidson, K., Gowen, R. J., Harrison, P. J., Fleming, L. E., Hoagland, P., & Moschonas, G. (2014). Anthropogenic nutrients and harmful algae in coastal waters. *Journal of*

Environmental Management, *146*, 206–216. https://doi.org/10.1016/j.jenvman.2014.07.002

De Vargas, C., Audic, S., Henry, N., Decelle, J., Mahé, F., Logares, R., Lara, E., Berney, C., Le Bescot, N., Probert, I., Carmichael, M., Poulain, J., Romac, S., Colin, S., Aury, J.-M., Bittner, L., Chaffron, S., Dunthorn, M., Engelen, S., … Velayoudon, D. (2015). Eukaryotic plankton diversity in the sunlit ocean. *Science*, *348*(6237), 1261605. https://doi.org/10.1126/science.1261605

Del Giorgio, P. A. (Ed.). (2005). *Respiration in aquatic ecosystems* (1. publ). Oxford Univ. Press.

Elferink, S., Neuhaus, S., Wohlrab, S., Toebe, K., Voß, D., Gottschling, M., Lundholm, N., Krock, B., Koch, B. P., Zielinski, O., Cembella, A., & John, U. (2017). Molecular diversity patterns among various phytoplankton size-fractions in West Greenland in late summer. *Deep Sea Research Part I: Oceanographic Research Papers*, *121*, 54–69. https://doi.org/10.1016/j.dsr.2016.11.002

Field, C. B., Behrenfeld, M. J., Randerson, J. T., & Falkowski, P. (1998). Primary Production of the Biosphere: Integrating Terrestrial and Oceanic Components. *Science*, *281*(5374), 237–240. https://doi.org/10.1126/science.281.5374.237

Foflonker, F., Ananyev, G., Qiu, H., Morrison, A., Palenik, B., Dismukes, G. C., & Bhattacharya, D. (2016). The unexpected extremophile: Tolerance to fluctuating salinity in the green alga Picochlorum. *Algal Research*, *16*, 465–472. https://doi.org/10.1016/j.algal.2016.04.003

Fournier, C., Fiedler, A., Weidele, M., Kautz, H., & Schleheck, D. (2024). Description of a 'plankton filtration bias' in sequencing-based bacterial community analysis and of an Arduino microcontroller-based flowmeter device that can help to resolve it. *PLOS ONE*, *19*(5), e0303937. https://doi.org/10.1371/journal.pone.0303937

Fredersdorf, J., Müller, R., Becker, S., Wiencke, C., & Bischof, K. (2009). Interactive effects of radiation, temperature and salinity on different life history stages of the Arctic kelp Alaria esculenta (Phaeophyceae). *Oecologia*, *160*(3), 483–492. https://doi.org/10.1007/s00442-009-1326-9

Froján, M., Muñoz-Colmenero, M., Teixeira, I. G., Arbones, B., Sotelo, C. G., Correa, B., Figueiras, F. G., & Castro, C. G. (2025). Unveiling Short-Scale Responses How Pico- and Nanoeukaryotic Plankton Navigate Environmental Variability in a Coastal Upwelling System. *Environmental Microbiology Reports*. https://doi.org/10.1111/1758-2229.70070

Fu, F., Tatters, A., & Hutchins, D. (2012). Global change and the future of harmful algal blooms in the ocean. *Marine Ecology Progress Series*, *470*, 207–233. https://doi.org/10.3354/meps10047

Fucikova, K., Leliaert, F., Cooper, E. D., Å kaloud, P., D'Hondt, S., De Clerck, O., Gurgel, C. F. D., Lewis, L. A., Lewis, P. O., Lopez-Bautista, J. M., Delwiche, C. F., & Verbruggen, H. (2014). New phylogenetic hypotheses for the core Chlorophyta based on chloroplast sequence data. *Frontiers in Ecology and Evolution*, *2*. https://doi.org/10.3389/fevo.2014.00063

GADM. (2022). GADM. https://gadm.org/download_country.html

Gasiūnaitė, Z. R., Cardoso, A. C., Heiskanen, A.-S., Henriksen, P., Kauppila, P., Olenina, I., Pilkaitytė, R., Purina, I., Razinkovas, A., Sagert, S., Schubert, H., & Wasmund, N. (2005). Seasonality of coastal phytoplankton in the Baltic Sea: Influence of salinity and eutrophication. *Estuarine, Coastal and Shelf Science*, *65*(1–2), 239–252. https://doi.org/10.1016/j.ecss.2005.05.018

GEBCO Bathymetric Compilation Group 2024. (2024). *The GEBCO_2024 Grid—A continuous terrain model of the global oceans and land.* (Version 1) [Binary,Delimited,Documents,Network Common Data Form]. NERC EDS British Oceanographic Data Centre NOC. https://doi.org/10.5285/1C44CE99-0A0D-5F4F-E063-7086ABC0EA0F

Glibert, P. M. (1998). Interactions of top-down and bottom-up control in planktonic nitrogen cycling. In T. Tamminen & H. Kuosa (Eds.), *Eutrophication in Planktonic Ecosystems: Food Web Dynamics and Elemental Cycling* (pp. 1–12). Springer Netherlands. https://doi.org/10.1007/978-94-017-1493-8_1

Gorokhova, O. G., & Zinchenko, T. D. (2025). Changes in the Size Structure of Algal Communities in Rivers of the Basin of Elton Lake under Salinity Gradient Conditions. *Arid Ecosystems*, *15*(3), 411–417. https://doi.org/10.1134/S2079096125700337

Gran-Stadniczenko, S., Egge, E., Hostyeva, V., Logaresc, R., Eikrem, W., & Edvardsena, B. (2018). Protist Diversity and Seasonal Dynamics in Skagerrak Plankton Communities as Revealed by Metabarcoding and Microscopy. *Journal of Eukaryotic Microbiology*. https://doi.org/doi:10.1111/jeu.12700

Grasshoff, K., Kremling, K., & Ehrhardt, M. (2009). *Methods of Seawater Analysis*. John Wiley & Sons.

Grattepanche, J.-D., Jeffrey, W. H., Gast, R. J., & Sanders, R. W. (2022). Diversity of Microbial Eukaryotes Along the West Antarctic Peninsula in Austral Spring. *Frontiers in Microbiology*, *13*, 844856. https://doi.org/10.3389/fmicb.2022.844856

Griffith, A. W., & Gobler, C. J. (2020). Harmful algal blooms: A climate change co-stressor in marine and freshwater ecosystems. *Harmful Algae*, *91*, 101590. https://doi.org/10.1016/j.hal.2019.03.008

Grimsley, N., Yau, S., Piganeau, G., & Moreau, H. (2015). Typical Features of Genomes in the Mamiellophyceae. In S. Ohtsuka, T. Suzaki, T. Horiguchi, N. Suzuki, & F. Not (Eds.), *Marine Protists* (pp. 107–127). Springer Japan. https://doi.org/10.1007/978-4-431-55130-0_6

Haider, D., Tolman, J., Beiko, R. G., & LaRoche, J. (2026). Comparison of Spatio-Temporal Dynamics and Composition in Size-Fractionated and Unfractionated Northwestern Atlantic Microbial Communities. *Environmental Microbiology Reports*, *18*(1), e70206. https://doi.org/10.1111/1758-2229.70206

Hallegraeff, G. M. (2010). OCEAN CLIMATE CHANGE, PHYTOPLANKTON COMMUNITY RESPONSES, AND HARMFUL ALGAL BLOOMS: A FORMIDABLE PREDICTIVE CHALLENGE. *Journal of Phycology*, *46*(2), 220–235. https://doi.org/10.1111/j.1529-8817.2010.00815.x

Hallegraeff, G. M., Anderson, D. M., & Cembella, A. D. (2003). *Manual on Harmful Marine Microalgae*. UNESCO Publishing.

Halpern, B. S., Walbridge, S., Selkoe, K. A., Kappel, C. V., Micheli, F., D'Agrosa, C., Bruno, J. F., Casey, K. S., Ebert, C., Fox, H. E., Fujita, R., Heinemann, D., Lenihan, H. S., Madin, E. M. P., Perry, M. T., Selig, E. R., Spalding, M., Steneck, R., & Watson, R. (2008). A Global Map of Human Impact on Marine Ecosystems. *Science*, *319*(5865), 948–952. https://doi.org/10.1126/science.1149345

Hartig, F., Lohse, L., & leite, M. de S. (2024). *DHARMa: Residual Diagnostics for Hierarchical (Multi-Level / Mixed) Regression Models* (Version 0.4.7) [Computer software]. https://cran.r-project.org/web/packages/DHARMa/index.html

Hassenrück, C. (2022). *Amplicon sequence processing workflow (paired-end mixed-orientation libraries generated at LGC Genomics)* (p. 115 kB) [Plain text (md, smk, R, sh, yaml), png]. Leibniz Institute for Baltic Sea Research Warnemünde (IOW). https://doi.org/10.12754/MISC-2022-0002

HELCOM, Raateoja, M., & Seppälä, J. (n.d.). *HELCOM Guidelines for monitoring of chlorophyll a.*

Herlemann, D. P. R., Labrenz, M., Jürgens, K., Bertilsson, S., Waniek, J. J., & Andersson, A. F. (2011). Transitions in bacterial communities along the 2000 km salinity gradient of the Baltic Sea. *The ISME Journal*, *5*(10), 1571–1579. https://doi.org/10.1038/ismej.2011.41

Hillebrand, H., Acevedo-Trejos, E., Moorthi, S. D., Ryabov, A., Striebel, M., Thomas, P. K., & Schneider, M. (2022). Cell size as driver and sentinel of phytoplankton community structure and functioning. *Functional Ecology*, *36*(2), 276–293. https://doi.org/10.1111/1365-2435.13986

Hu, Y. O. O., Karlson, B., Charvet, S., & Andersson, A. F. (2016). Diversity of Pico- to Mesoplankton along the 2000 km Salinity Gradient of the Baltic Sea. *Frontiers in Microbiology*, *7*. https://doi.org/10.3389/fmicb.2016.00679

Irwin, A. J., Finkel, Z. V., Schofield, O. M. E., & Falkowski, P. G. (2006). Scaling-up from nutrient physiology to the size-structure of phytoplankton communities. *Journal of Plankton Research*, *28*(5), 459–471. https://doi.org/10.1093/plankt/fbi148

Jacquet, S., Partensky, F., Lennon, J., & Vaulot, D. (2001). DIEL PATTERNS OF GROWTH AND DIVISION IN MARINE PICOPLANKTON IN CULTURE. *Journal of Phycology*, *37*(3), 357–369. https://doi.org/10.1046/j.1529-8817.2001.037003357.x

Jänes, H., Herkül, K., & Kotta, J. (2017). Environmental niche separation between native and non-native benthic invertebrate species: Case study of the northern Baltic Sea. *Marine Environmental Research*, *131*, 123–133. https://doi.org/10.1016/j.marenvres.2017.08.001

Jimenez, V., & Burns, J. A. (2021). No Evidence of Phago-Mixotrophy in Micromonas polaris (Mamiellophyceae), the dominant Picophytoplankton Species in the Arctic. *Journal of Phycology*.

Karp-Boss, L., Boss, E., & Jumars, P. A. (1996). *NUTRIENT FLUXES TO PLANKTONIC OSMOTROPHS IN THE PRESENCE OF FLUID MOTION*.

Klais, R., Tamminen, T., Kremp, A., Spilling, K., An, B. W., Hajdu, S., & Olli, K. (2013). Spring phytoplankton communities shaped by interannual weather variability and dispersal limitation: Mechanisms of climate change effects on key coastal primary producers. *Limnology and Oceanography*, *58*(2), 753–762. https://doi.org/10.4319/lo.2013.58.2.0753

Klais, R., Tamminen, T., Kremp, A., Spilling, K., & Olli, K. (2011). Decadal-Scale Changes of Dinoflagellates and Diatoms in the Anomalous Baltic Sea Spring Bloom. *PLoS ONE*, *6*(6), e21567. https://doi.org/10.1371/journal.pone.0021567

Köster, J. (2024). *Data analysis for paper "Sustainable data analysis with Snakemake."* Zenodo. https://doi.org/10.5281/ZENODO.4244143

Kulakova, N. V., Kashin, S. A., & Bukin, Y. S. (2020). The genetic diversity and phylogeny of green microalgae in the genus Choricystis (Trebouxiophyceae, Chlorophyta) in Lake Baikal. *Limnology*, *21*(1), 15–24. https://doi.org/10.1007/s10201-019-00587-x

Lampe, R. (2022). The lithostratigraphic formations of the coastal Holocene in NE Germany – a synthesis. *E&G Quaternary Science Journal*, *71*(2), 249–265. https://doi.org/10.5194/egqsj-71-249-2022

Landesamt für Umwelt, Naturschutz und Geologie. (n.d.). *WRRL Wasserkörper-Steckbrief Küstengewässer Mecklenburg-Vorpommern: Bewirtschaftungszeitraum 2022–2027.* Retrieved December 31, 2025, from https://fis-wasser-mv.de/charts/steckbriefe/cw/cw_wk.php?kg=WP_13

Lefranc, M., Thénot, A., Lepère, C., & Debroas, D. (2005). Genetic Diversity of Small Eukaryotes in Lakes Differing by Their Trophic Status. *Applied and Environmental Microbiology*, *71*(10), 5935–5942. https://doi.org/10.1128/AEM.71.10.5935-5942.2005

Legendre, L., & Le Fèvre, J. (1995). Microbial food webs and the export of biogenic carbon in oceans. *Aquatic Microbial Ecology*, *9*, 69–77. https://doi.org/10.3354/ame009069

Lenth, R. V., Piaskowski, J., Banfai, B., Bolker, B., Buerkner, P., Giné-Vázquez, I., Hervé, M., Jung, M., Love, J., Miguez, F., Riebl, H., & Singmann, H. (2026). *emmeans: Estimated Marginal Means, aka Least-Squares Means* (Version 2.0.2) [Computer software]. https://cran.r-project.org/web/packages/emmeans/index.html

Mangot, J.-F., Domaizon, I., Taib, N., Marouni, N., Duffaud, E., Bronner, G., & Debroas3, D. (2013). Short-term dynamics of diversity patterns: Evidence of continual reassembly within lacustrine small eukaryotes. *Environmental Microbiology*, 1745–1758. https://doi.org/10.1111/1462-2920.12065

Mangot, J.-F., Lepère, C., Bouvier, C., Debroas, D., & Domaizon, I. (2009). Community Structure and Dynamics of Small Eukaryotes Targeted by New Oligonucleotide Probes: New Insight into the Lacustrine Microbial Food Web. *Applied and Environmental Microbiology*, *75*(19), 6373–6381. https://doi.org/10.1128/AEM.00607-09

Martin, M. (2011). Cutadapt removes adapter sequences from high-throughput sequencing reads. *EMBnet.Journal*, *17*(1), 10–12. https://doi.org/10.14806/ej.17.1.200

Massana, R. (2011). Eukaryotic Picoplankton in Surface Oceans. *Annual Review of Microbiology*, *65*(1), 91–110. https://doi.org/10.1146/annurev-micro-090110-102903

Massana, R., Gobet, A., Audic, S., Bass, D., Bittner, L., Boutte, C., Chambouvet, A., Christen, R., Claverie, J., Decelle, J., Dolan, J. R., Dunthorn, M., Edvardsen, B., Forn, I., Forster, D., Guillou, L., Jaillon, O., Kooistra, W. H. C. F., Logares, R., … De Vargas, C. (2015). Marine protist diversity in European coastal waters and sediments as revealed by high-throughput sequencing. *Environmental Microbiology*, *17*(10), 4035–4049. https://doi.org/10.1111/1462-2920.12955

Mazur-Marzec, H., Andersson, A. F., Błaszczyk, A., Dąbek, P., Górecka, E., Grabski, M., Jankowska, K., Jurczak-Kurek, A., Kaczorowska, A. K., Kaczorowski, T., Karlson, B., Kataržytė, M., Kobos, J., Kotlarska, E., Krawczyk, B., Łuczkiewicz, A., Piwosz, K., Rybak, B., Rychert, K., … Węgrzyn, A. (2024). Biodiversity of microorganisms in the Baltic Sea: The power of novel methods in the identification of marine microbes. *FEMS Microbiology Reviews*, *48*(5), fuae024. https://doi.org/10.1093/femsre/fuae024

McKie-Krisberg, Z. M., & Sanders, R. W. (2014). Phagotrophy by the picoeukaryotic green alga *Micromonas*: Implications for Arctic Oceans. *The ISME Journal*, *8*(10), 1953–1961. https://doi.org/10.1038/ismej.2014.16

McMurdie, P. J., & Holmes, S. (2013). phyloseq: An R package for reproducible interactive analysis and graphics of microbiome census data. *PLoS ONE*, *8*(4), e61217.

McQuatters-Gollop, A., Stern, R. F., Atkinson, A., Best, M., Bresnan, E., Creach, V., Devlin, M., Holland, M., Ostle, C., Schmidt, K., Sheppard, L., Tarran, G., Woodward, E. M. S., & Tett, P. (2024). The silent majority: Pico- and nanoplankton as ecosystem health indicators for marine policy. *Ecological Indicators*, *159*, 111650. https://doi.org/10.1016/j.ecolind.2024.111650

Mitra, A., Flynn, K. J., Burkholder, J. M., Berge, T., Calbet, A., Raven, J. A., Granéli, E., Glibert, P. M., Hansen, P. J., Stoecker, D. K., Thingstad, F., Tillmann, U., Våge, S., Wilken, S., & Zubkov, M. V. (2014). The role of mixotrophic protists in the biological carbon pump. *Biogeosciences*, *11*(4), 995–1005. https://doi.org/10.5194/bg-11-995-2014

Moore, S. K., Trainer, V. L., Mantua, N. J., Parker, M. S., Laws, E. A., Backer, L. C., & Fleming, L. E. (2008). Impacts of climate variability and future climate change on harmful algal blooms and human health. *Environmental Health*, *7*(Suppl 2), S4. https://doi.org/10.1186/1476-069X-7-S2-S4

Müller, F., Baessler, C., Schubert, H., & Klotz, S. (Eds.). (2010). *Long-Term Ecological Research*. Springer Netherlands. https://doi.org/10.1007/978-90-481-8782-9

Munkes, B. (2005). Eutrophication, phase shift, the delay and the potential return in the Greifswalder Bodden, Baltic Sea. *Aquatic Sciences*, *67*(3), 372–381. https://doi.org/10.1007/s00027-005-0761-x

Nagarkar, M., Countway, P. D., Du Yoo, Y., Daniels, E., Poulton, N. J., & Palenik, B. (2018). Temporal dynamics of eukaryotic microbial diversity at a coastal Pacific site. *The ISME Journal*, *12*(9), 2278–2291. https://doi.org/10.1038/s41396-018-0172-3

NOAA. (2024, June 16). *Why do harmful algal blooms occur?* [National Ocean Service website]. https://oceanservice.noaa.gov/facts/why_habs.html

Oksanen, J., Simpson, G. L., Blanchet, F. G., Kindt, R., Legendre, P., Minchin, P. R., O'Hara, R. B., Solymos, P., Stevens, M. H. H., Szoecs, E., Wagner, H., Barbour, M., Bedward, M., Bolker, B., Borcard, D., Borman, T., Carvalho, G., Chirico, M., De Caceres, M., … Weedon, J. (2025). *vegan: Community Ecology Package*. https://doi.org/10.32614/CRAN.package.vegan

Olli, K., Nyman, E., & Tamminen, T. (2023). Half-century trends in alpha and beta diversity of phytoplankton summer communities in the Helsinki Archipelago, the Baltic Sea. *Journal of Plankton Research*, *45*(1), 146–162. https://doi.org/10.1093/plankt/fbac029

Olofsson, M., Hagan, J. G., Karlson, B., & Gamfeldt, L. (2020). Large seasonal and spatial variation in nano- and microphytoplankton diversity along a Baltic Sea—North Sea salinity gradient. *Scientific Reports*, *10*(1), 17666. https://doi.org/10.1038/s41598-020-74428-8

Ortiz-Álvarez, R., Triadó-Margarit, X., Camarero, L., Casamayor, E. O., & Catalan, J. (2018). High planktonic diversity in mountain lakes contains similar contributions of autotrophic, heterotrophic and parasitic eukaryotic life forms. *Scientific Reports*, *8*(1), 4457. https://doi.org/10.1038/s41598-018-22835-3

Pawlowski, J., Audic, S., Adl, S., Bass, D., Belbahri, L., Berney, C., Bowser, S. S., Cepicka, I., Decelle, J., Dunthorn, M., Fiore-Donno, A. M., Gile, G. H., Holzmann, M., Jahn, R., Jirků, M., Keeling, P. J., Kostka, M., Kudryavtsev, A., Lara, E., … De Vargas, C. (2012). CBOL Protist Working Group: Barcoding Eukaryotic Richness beyond the Animal, Plant, and Fungal Kingdoms. *PLoS Biology*, *10*(11), e1001419. https://doi.org/10.1371/journal.pbio.1001419

Pedersen, T. L. (2025). *patchwork: The Composer of Plots* (Version 1.3.2) [Computer software]. https://cran.r-project.org/web/packages/patchwork/index.html

Piwosz, K., Całkiewicz, J., Gołębiewski, M., & Creer, S. (2018). Diversity and community composition of pico- and nanoplanktonic protists in the Vistula River estuary (Gulf of

Gdańsk, Baltic Sea). *Estuarine, Coastal and Shelf Science*, *207*, 242–249. https://doi.org/10.1016/j.ecss.2018.04.013

Prokopowich, C. D., Gregory, T. R., & Crease, T. J. (2003). The correlation between rDNA copy number and genome size in eukaryotes. *Genome*, *46*(1), 48–50.

R Core Team. (2025). *R: A language and environment for statistical computing*. https://www.r-project.org/

Raven, J. A. (1998). The twelfth Tansley Lecture. Small is beautiful: The picophytoplankton. *Functional Ecology*, *12*(4), 503–513. https://doi.org/10.1046/j.1365-2435.1998.00233.x

Rojas-Jimenez, K., Rieck, A., Wurzbacher, C., Jürgens, K., Labrenz, M., & Grossart, H.-P. (2019). A Salinity Threshold Separating Fungal Communities in the Baltic Sea. *Frontiers in Microbiology*, *10*, 680. https://doi.org/10.3389/fmicb.2019.00680

Ryabov, A., Kerimoglu, O., Litchman, E., Olenina, I., Roselli, L., Basset, A., Stanca, E., & Blasius, B. (2021). Shape matters: The relationship between cell geometry and diversity in phytoplankton. *Ecology Letters*, *24*(4), 847–861. https://doi.org/10.1111/ele.13680

Salis, R., & Hansson, L.-A. (2025). Comparative Analysis of Environmental DNA Metabarcoding and Spectro-Fluorescence for Phytoplankton Community Assessments. *Environmental DNA*. https://doi.org/10.1002/edn3.70097

Sassenhagen, I., Herlemann, D. P. R., Gentsch, K., Kremp, A., Labrenz, M., & Dutz, J. (2025). The impact of temperature and sediment resuspension on microbial eukaryote recruitment from shallow Baltic Sea sediment. *Frontiers in Microbiology*, *16*, 1654505. https://doi.org/10.3389/fmicb.2025.1654505

Schiewer, U. (2001). *Salzhaff, Greifswalder Bodden, Darß-Zingster Boddenkette: Gewässereutrophierung und Pufferkapazität – ein Vergleich*.

Schiewer, U. (2008). *Ecology of Baltic coastal waters*. Springer.

Sehein, T. R., Gast, R. J., Pachiadaki, M., Guillou, L., & Edgcomb, V. P. (2022). Parasitic infections by Group II Syndiniales target selected dinoflagellate host populations within diverse protist assemblages in a model coastal pond. *Environmental Microbiology*, *24*(4), 1818–1834. https://doi.org/10.1111/1462-2920.15977

Sieburth, J. M., Smetacek, V., & Lenz, J. (1978). Pelagic ecosystem structure: Heterotrophic compartments of the plankton and their relationship to plankton size fractions. *Limnology and Oceanography*, *23*(6), 1256–1263. https://doi.org/10.4319/lo.1978.23.6.1256

Siegel, H., Gerth, M., & Tschersich, G. (2006). Sea surface temperature development of the Baltic Sea in the period 1990–2004. *Oceanologia*, *48*, 119–131.

Sildever, S., Laas, P., Kolesova, N., Lips, I., Lips, U., & Nagai, S. (2021). Plankton biodiversity and species co-occurrence based on environmental DNA – a multiple marker study. *Metabarcoding and Metagenomics*, *5*, e72371. https://doi.org/10.3897/mbmg.5.72371

Skovgaard, A. (2014). *Dirty Tricks in the Plankton: Diversity and Role of Marine Parasitic Protists*. https://doi.org/10.4467/16890027AP.14.006.1443

Slaveykova, V., Sonntag, B., & Gutiérrez, J. C. (2016). Stress and Protists: No life without stress. *European Journal of Protistology*, *55*, 39–49. https://doi.org/10.1016/j.ejop.2016.06.001

Stoeck, T., Bass, D., Nebel, M., Christen, R., Jones, M. D. M., Breiner, H., & Richards, T. A. (2010). Multiple marker parallel tag environmental DNA sequencing reveals a highly complex eukaryotic community in marine anoxic water. *Molecular Ecology*, *19*(s1), 21–31. https://doi.org/10.1111/j.1365-294X.2009.04480.x

Stoecker, D., Johnson, M., deVargas, C., & Not, F. (2009). Acquired phototrophy in aquatic protists. *Aquatic Microbial Ecology*, *57*, 279–310. https://doi.org/10.3354/ame01340

Tange, O. (2011). *GNU Parallel: The Command-Line Power Tool*.

Telesh, I., Schubert, H., & Skarlato, S. (2011). Revisiting Remane's concept: Evidence for high plankton diversity and a protistan species maximum in the horohalinicum of the Baltic Sea. *Marine Ecology Progress Series*, *421*, 1–11. https://doi.org/10.3354/meps08928

Telesh, I., Schubert, H., & Skarlato, S. (2013). Life in the salinity gradient: Discovering mechanisms behind a new biodiversity pattern. *Estuarine, Coastal and Shelf Science*, *135*, 317–327. https://doi.org/10.1016/j.ecss.2013.10.013

Tozzi, Schofield, O., & Falkowski, P. (2004). *Historical climate change and ocean turbulence as selective agents for two key phytoplankton functional groups*. *Vol. 274*, 123–132.

Tragin, M., Lopes Dos Santos, A., Christen, R., & Vaulot, D. (2016). Diversity and ecology of green microalgae in marine systems: An overview based on 18S rRNA gene sequences. *Perspectives in Phycology*, *3*(3), 141–154. https://doi.org/10.1127/pip/2016/0059

Tragin, M., & Vaulot, D. (2019). Novel diversity within marine Mamiellophyceae (Chlorophyta) unveiled by metabarcoding. *Scientific Reports*, *9*(1), 5190. https://doi.org/10.1038/s41598-019-41680-6

Turmel, M., Otis, C., & Lemieux, C. (2020). Complete mitogenome of the chlorophyte green alga *Marsupiomonas* sp. NIES 1824 (Pedinophyceae). *Mitochondrial DNA Part B*, *5*(1), 548–550. https://doi.org/10.1080/23802359.2019.1710283

Vaulot, D., del Campo, J., Pohl, N., Salomaki, E., Gu, H., Bonacolta, A., Morard, R., Krabberød, A. K., Arañó Ansola, J., & Селюк, A. (2025). *PR2 version 5.1.0—Data* [Dataset]. Zenodo. https://doi.org/10.5281/zenodo.15129782

Vaulot, D., & Marie, D. (1999). Diel variability of photosynthetic picoplankton in the equatorial Pacific. *Journal of Geophysical Research: Oceans*, *104*(C2), 3297–3310. https://doi.org/10.1029/98JC01333

Viitasalo, M., & Bonsdorff, E. (2022). Global climate change and the Baltic Sea ecosystem: Direct and indirect effects on species, communities and ecosystem functioning. *Earth System Dynamics*, *13*(2), 711–747. https://doi.org/10.5194/esd-13-711-2022

Wang, F., Xie, Y., Wu, W., Sun, P., Wang, L., & Huang, B. (2019). Picoeukaryotic Diversity And Activity in the Northwestern Pacific Ocean Based on rDNA and rRNA High-Throughput Sequencing. *Frontiers in Microbiology*, *9*, 3259. https://doi.org/10.3389/fmicb.2018.03259

Wang, L., Wang, S., Wang, L., Sun, D., Lang, S., Jia, Y., & Zhang, H. (2026). Estimating Global Marine Size-Fractionated Primary Productivity Over Two Decades Using a Depth-Independent Model. *Global Biogeochemical Cycles*. https://doi.org/10.1029/2025GB008851

Wasmund, N., Nausch, G., & Matthäus, W. (1998). Phytoplankton spring blooms in the southern Baltic Sea—Spatio-temporal development and long-term trends. *Journal of Plankton Research*, *20*(6), 1099–1117. https://doi.org/10.1093/plankt/20.6.1099

Wickham, H. (2016). ggplot2: Elegant Graphics for Data Analysis. *Springer-Verlag New York*. https://ggplot2.tidyverse.org

Wickham, H., Averick, M., Bryan, J., Chang, W., D'Agostino McGowan, L., Francois, R., Grolemund, G., Hayes, A., Henry, L., Hester, J., Kuhn, M., Pedersen, T. L., Miller, E., Bache, S. M., Müller, K., Ooms, J., Robinson, D., Seidel, D. P., Spinu, V., … Yutani, H. (2019). Welcome to the {tidyverse}. *Journal of Open Source Software*, *4*(43), 1686. https://doi.org/10.21105/joss.01686

Wickham, H., Francois, R., Henry, L., Müller, K., & Vaughan, D. (2023). *dplyr: A Grammar of Data Manipulation.* https://doi.org/10.32614/CRAN.package.dplyr

Worden, A. Z., Follows, M. J., Giovannoni, S. J., Wilken, S., Zimmerman, A. E., & Keeling, P. J. (2015). Rethinking the marine carbon cycle: Factoring in the multifarious lifestyles of microbes. *Science*, *347*(6223), 1257594. https://doi.org/10.1126/science.1257594

Wu, W., & Liu, H. (2022). Cell size is a key ecological trait associated with biogeographic patterns of microbial eukaryotes in coastal waters. *Frontiers in Marine Science*, *9*, 933256. https://doi.org/10.3389/fmars.2022.933256

Xu, Q., Wang, C., Xu, K., & Chen, N. (2021). Metabarcoding Analysis of Harmful Algal Bloom Species in the Western Pacific Seamount Regions. *International Journal of Environmental Research and Public Health*, *18*(21), 11470. https://doi.org/10.3390/ijerph182111470

Xu, Z., Wang, M., Wu, W., Li, Y., Liu, Q., Han, Y., Jiang, Y., Shao, H., McMinn, A., & Liu, H. (2018). Vertical Distribution of Microbial Eukaryotes From Surface to the Hadal Zone of the Mariana Trench. *Frontiers in Microbiology*, *9*, 2023. https://doi.org/10.3389/fmicb.2018.02023

Zheng, X., Guo, X., Lin, X., & Huang, L. (2025). Contrasting patterns in diversity and community assembly of bacterioplankton and three size fractions of protists in the South China Sea. *Applied and Environmental Microbiology*, *91*(7), e00436-25. https://doi.org/10.1128/aem.00436-25

Zuur, A. F., Ieno, E. N., & Elphick, C. S. (2010). A protocol for data exploration to avoid common statistical problems: *Data exploration*. *Methods in Ecology and Evolution*, *1*(1), 3–14. https://doi.org/10.1111/j.2041-210X.2009.00001.x

Abbreviations

µm	Micrometer
ASV	Amplicon Sequence Variant
BCP	Biological Carbon Pump
BfN	Bundesamt für Naturschutz (The German Federal Agency for Nature Conservation)
Bp	Base Pair
Chl *a*	Chlorophyll *a*
CTD	Conductivity–Temperature–Depth
ddPCR	Droplet Digital Polymerase Chain Reaction
eDNA	Environmental DNA
GLMM	Generalized Linear Mixed Model
GWB	Greifswalder Bodden
LMM	Linear Mixed Model
Loess	Locally Estimated Scatterplot Smoothing
MCE	Mixed Cellulose Esters
NMDS	Non-metric Multidimensional Scaling
PCR	Polymerase Chain Reaction
PR2	Protist Ribosomal Reference
PSU	Practical Salinity Units
QC	Quality Control
qPCR	Quantitative Polymerase Chain Reaction
SD	Standard Deviation
SDA	Standard Data Acquisition
SE	Standard Error
VIF	Variance Inflation Factors

Appendix

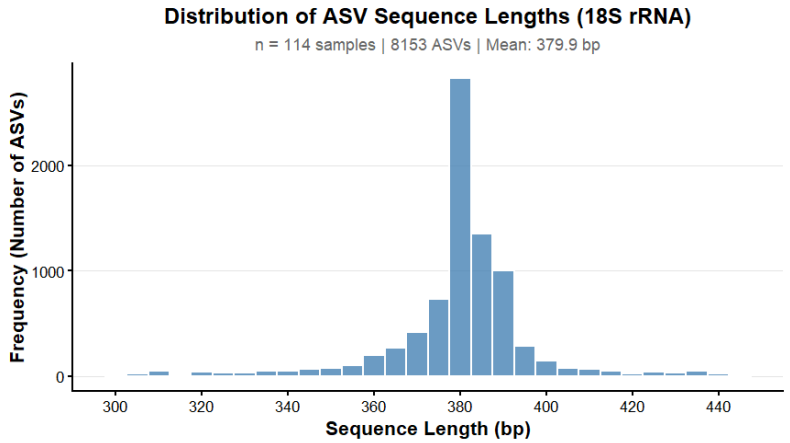

Figure S 1: Distribution of ASV sequence lengths for 18S rRNA amplicons before the quality control (QC) filtering steps. The x-axis shows the sequence length in base pairs (bp) and the y-axis shows the frequency (number of ASVs). The mean is 379.9 bp for the total of 114 samples.

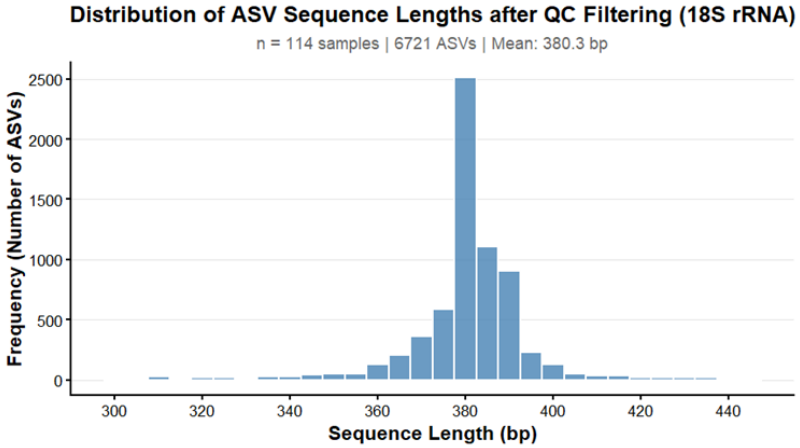

Figure S 2: Distribution of ASV sequence lengths for 18S rRNA amplicons after the quality control (QC) filtering steps. The x-axis shows the sequence length in base pairs (bp) and the y-axis shows the frequency (number of ASVs). The mean is 380.3 bp for the total of 114 samples.

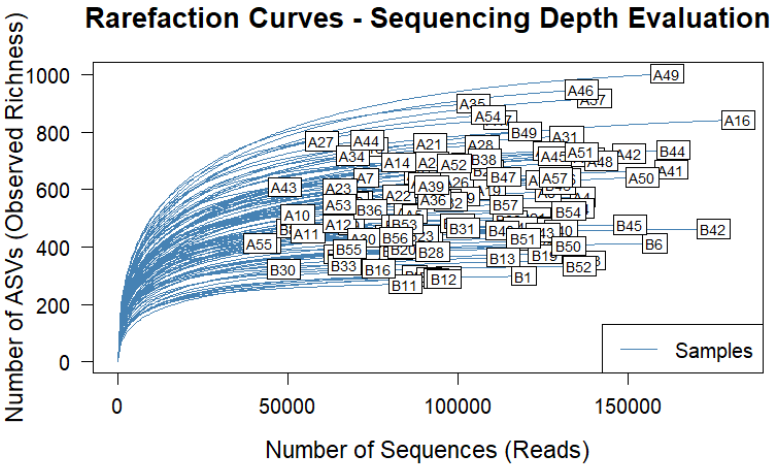

Figure S 3: Rarefaction curves for all samples. The x-axis shows the number of sequences (in reads) and the y-axis shows the number of ASVs (observed richness). Each blue line represents one sample.

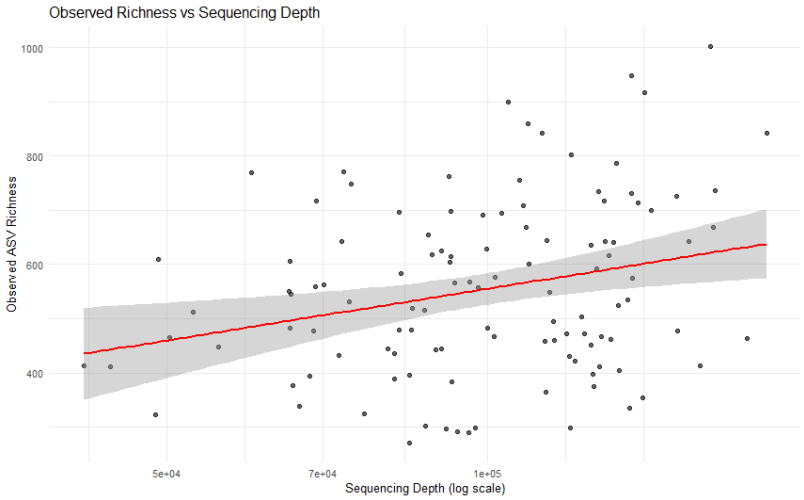

Figure S 4: Relationship between sequencing depth and observed ASV richness across all samples (n = 114). The red line indicates a linear regression fit with 95% confidence interval. Spearman's $\rho = 0.24$, $p = 0.009$.

Table S 1: Results of the quantitative slope analysis for evaluating sequence depth saturation. The five samples with the best saturation (lowest slope of the rarefaction curve at the endpoint) are shown. The total number of reads per sample, the final slope of the curve, and the number of newly discovered ASVs per 1,000 additional reads are indicated. A low slope (close to zero) indicates that microbial diversity was almost completely covered by the existing sequencing depth.

Sample	Total Reads	Slope	New ASVs per 1,000 Reads
B45	150,712	0.00010	0.100
B42	175,233	0.00010	0.103
B52	135,786	0.00015	0.148
B39	115,331	0.00016	0.157
B34	127,770	0.00016	0.165

Table S 2: Results of the quantitative slope analysis for evaluating sequence depth saturation. The five samples with the worst saturation (lowest slope of the rarefaction curve at the endpoint) are shown. The total number of reads per sample, the final slope of the curve, and the number of newly discovered ASVs per 1,000 additional reads are indicated. Higher slope values indicate that the microbial diversity in these specific samples may not been fully exhausted by the current sequencing depth.

Sample	Total Reads	Slope	New ASVs per 1,000 Reads
A27	60,074	0.00117	1.168
A2	44,257	0.00118	1.180
A10	52,907	0.00122	1.218
A53	65,117	0.00125	1.246
A44	73,282	0.00141	1.411

Table S 3: Missing Environmental Data Summary. Number of missing samples for each environmental variable in the entire data set (n = 114 samples).

Environmental Variable	Missing Samples	% Missing
Temperature (°C)	6	5.3
Salinity (PSU)	6	5.3
Dissolved Oxygen (mg/L)	6	5.3
Phosphate (µmol/L)	4	3.5
Nitrate (µmol/L)	4	3.5
Chlorophyll *a* (mg/m³)	4	3.5
Silicate (µmol/L)	4	3.5
Nitrite (µmol/L)	4	3.5
Ammonium (µmol/L)	4	3.5
Secchi depth (m)	20	17.5

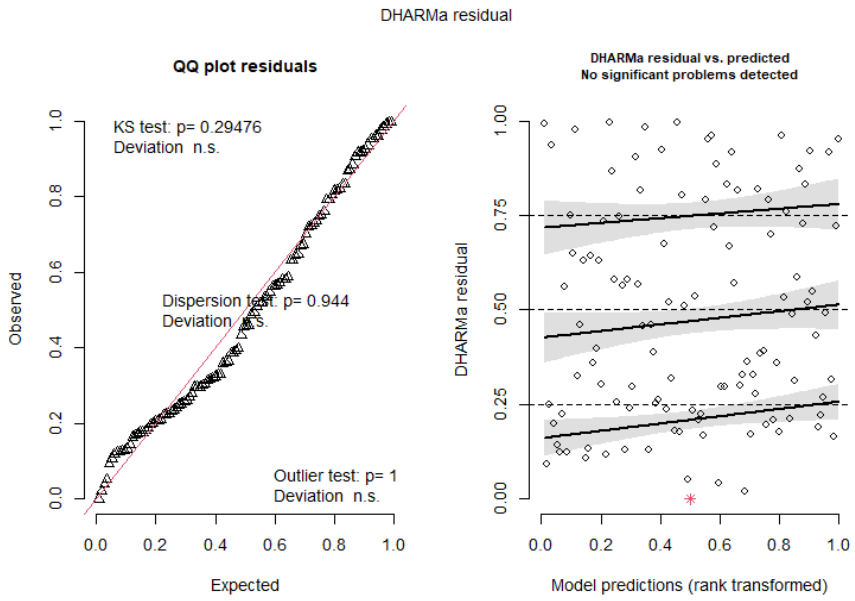

Figure S 5: DHARMa residual diagnosis of the GLMM for observed ASV richness. (Left) QQ plot of the simulated residuals: The observed residuals closely follow the expected uniform distribution (red line). The Kolmogorov-Smirnov test shows no significant deviation from uniform distribution (KS test: p = 0.29476, n.s.), the dispersion test confirms no over- or underdispersion (p = 0.944, n.s.), and the outlier test identifies no influential data points (p = 1, n.s.). (Right) Residuals vs. model predictors.

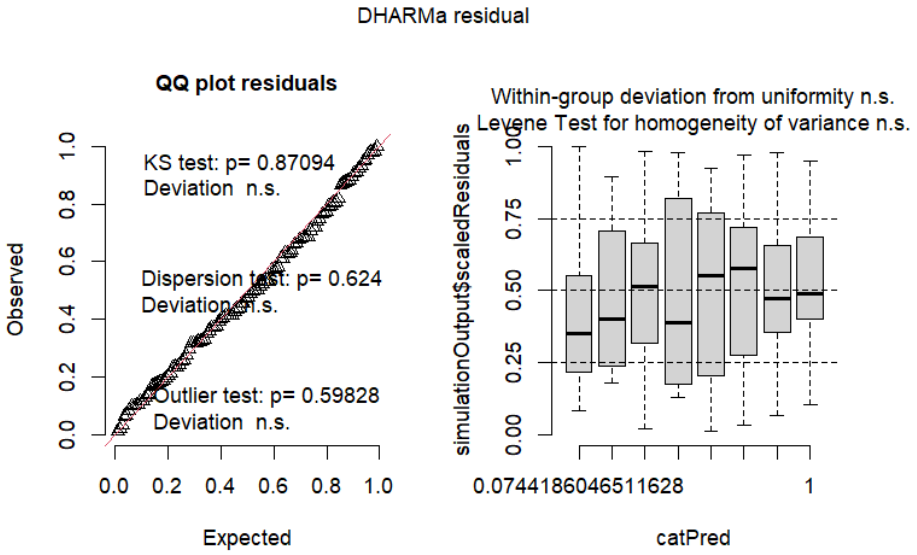

Figure S 6: DHARMa residual diagnosis of the LMM for the Shannon diversity index. (Left) QQ plot of the simulated residuals: The observed residuals follow the expected uniform distribution without any discernible systematic deviations (red line). The Kolmogorov-Smirnov test shows no significant deviation from uniform distribution (KS test: $p = 0.87094$, n.s.), the dispersion test confirms neither over- nor underdispersion ($p = 0.624$, n.s.), and the outlier test identifies no influential data points ($p = 0.59828$, n.s.). (Right) Residuals vs. categorical predictors (catPred): The box plots of the scaled residuals are evenly distributed around 0.5 across all three predictor groups, with no systematic shifts.

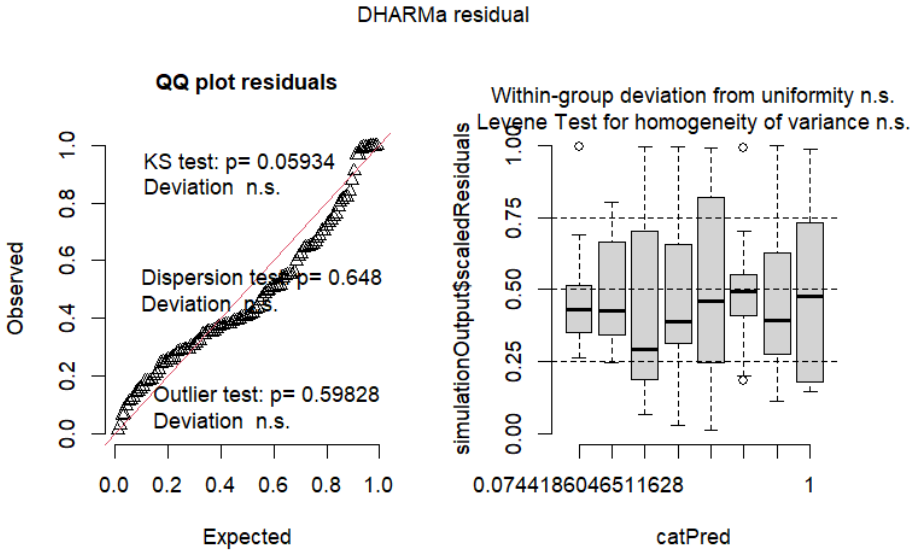

Figure S 7: DHARMa residual diagnosis of the LMM for the inverse Simpson diversity index. (Left) QQ plot of the simulated residuals: The observed residuals deviate slightly from the expected uniform distribution (red line) in the upper range, but remain acceptably close to the theoretical distribution overall. The Kolmogorov-Smirnov test shows no significant deviation (KS test: $p = 0.05934$, n.s.), the dispersion test confirms no over- or underdispersion ($p = 0.648$, n.s.), and the outlier test identifies no influential data points ($p = 0.59828$, n.s.). (Right) Residuals vs. categorical predictors (catPred): The box plots of the scaled residuals are distributed fairly evenly around 0.5 across all three predictor groups; individual outliers (open circles) were identified but do not exceed critical thresholds.

Table S 4: Random Effects (Variance Components). This table summarizes the variance and standard deviation (SD) attributed to the random effect of 'Station' and 'Water Sample' for each diversity model. Near-zero variance estimates indicate that the corresponding grouping factor explained little additional variation in the respective diversity metric.

Model	Random Effect	Variance	SD
Observed	Water Sample	0.01539	0.12404
Observed	Station	0.00371	0.06094
Shannon	Water Sample	0.00304	0.05511
Shannon	Station	0	0
Inv. Simpson	Water Sample	3.25463	1.80406
Inv. Simpson	Station	0.00000013	0.00037

Table S 5: Complete pairwise Comparisons of Temporal Succession for the large size fraction (≥5 µm). Results of post-hoc pairwise comparisons between sampling weeks. The table displays estimated differences (Estimate), standard errors (SE), test statistics (*z* ratios for GLMM or *t* ratios for LMM), and adjusted *p*-values for each diversity index. Note: All *p*-values were adjusted using the Benjamini-Hochberg (BH) method. Estimates for Observed ASV Richness are on the log scale. Significance levels: *** $p < 0.001$; ** $p < 0.01$; * $p < 0.05$; ns: not significant ($p > 0.05$).

Comparison	Index	Estimate	SE	Test Statistics	*p* (adj.)
W1 - W2	Observed	-0.125	0.065	z = −1.93	0.141 (ns)
	Shannon	-0.061	0.109	t = −0.56	0.693 (ns)
	Inv. Simp.	0.470	2.330	t = 0.20	0.912 (ns)
W1 - W3	Observed	-0.120	0.066	z = −1.81	0.141 (ns)
	Shannon	0.002	0.109	t = 0.01	0.989 (ns)
	Inv. Simp.	-0.258	2.330	t = −0.11	0.912 (ns)
W1 - W4	Observed	-0.162	0.067	z = −2.43	0.092 (ns)
	Shannon	0.135	0.109	t = 1.24	0.462 (ns)
	Inv. Simp.	3.130	2.330	t = 1.34	0.529 (ns)
W2 - W3	Observed	-0.005	0.065	z = 0.08	0.938 (ns)
	Shannon	0.063	0.111	t = 0.56	0.693 (ns)
	Inv. Simp.	-0.728	2.370	t = −0.31	0.912 (ns)
W2 - W4	Observed	-0.037	0.066	z = −0.56	0.687 (ns)
	Shannon	0.197	0.111	t = 1.77	0.462 (ns)
	Inv. Simp.	2.660	2.370	t = 1.12	0.529 (ns)
W3 - W4	Observed	-0.042	0.065	z = −0.65	0.687 (ns)
	Shannon	0.134	0.111	t = 1.21	0.462 (ns)
	Inv. Simp.	3.387	2.370	t = 1.43	0.529 (ns)

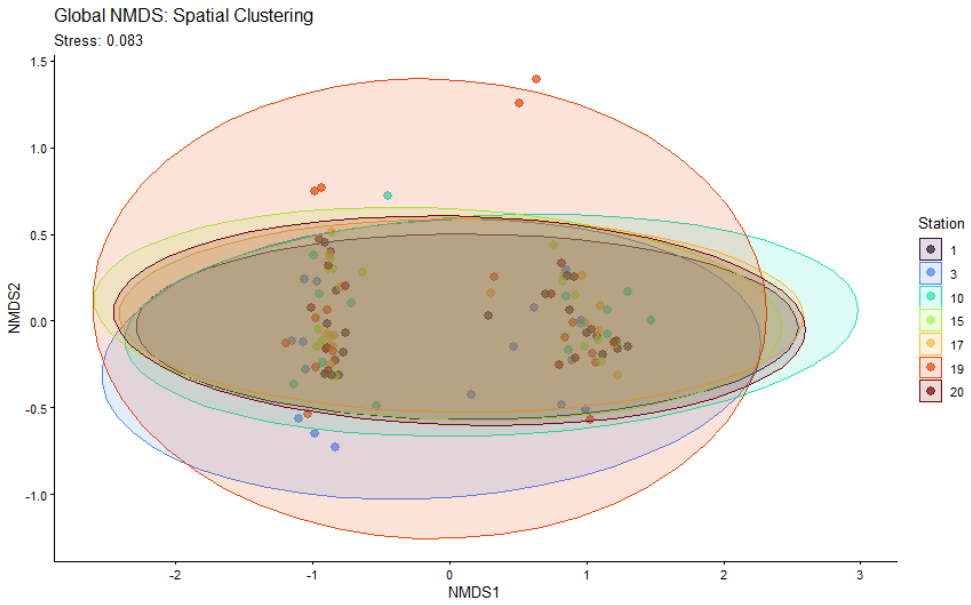

Figure S 8: Non-metric multidimensional scaling (NMDS) of the global microbial community structure according to sampling stations. The ordination is based on Bray-Curtis dissimilarities of relative ASV abundances and shows the spatial distribution across all samples. The samples are color-coded according to the seven sampling stations. Ellipses represent the 95% confidence interval for each station. k = 2 dimensions, stress = 0.083.

Table S 6: Results of the Permutational Multivariate Analysis of Variance (PERMANOVA). The marginal effects of environmental parameters on microbial community structure (based on Bray-Curtis distances of relative abundance data) are shown. To account for the repeated measures design and spatial dependency, permutations (n = 999) were blocked within stations. The table lists the degrees of freedom (*df*), sums of squares, the proportion of explained variance (R^2), the *F*-statistic, and the *p*-value (*Pr*(>*F*)). Significance levels: ** $p < 0.01$; * $p < 0.05$; . $p < 0.1$; ns: not significant ($p > 0.05$).

Environm. Parameter	Fraction	*df*	Sum of Squares	R^2	*F*	*Pr*(>*F*)
Nitrite	≥5 µm	1	0.277	0.044	2.417	**0.033** *
	0.22-5 µm	1	0.176	0.025	1.444	0.206 (ns)
Ammonium	≥5 µm	1	0.246	0.039	2.148	0.061 .
	0.22-5 µm	1	0.126	0.018	1.038	0.532 (ns)
Salinity	≥5 µm	1	0.088	0.014	0.764	0.610 (ns)
	0.22-5 µm	1	0.154	0.022	1.264	0.214 (ns)
Dissolved Oxygen	≥5 µm	1	0.104	0.016	0.909	0.492 (ns)
	0.22-5 µm	1	0.441	0.063	3.624	**0.004** **
Temperature	≥5 µm	1	0.085	0.013	0.738	0.831 (ns)
	0.22-5 µm	1	0.124	0.018	1.019	0.493 (ns)
Nitrate	≥5 µm	1	0.135	0.021	1.174	0.351 (ns)
	0.22-5 µm	1	0.21	0.03	1.726	0.165 (ns)
Chlorophyll *a*	≥5 µm	1	0.074	0.012	0.646	0.671 (ns)
	0.22-5 µm	1	0.101	0.014	0.828	0.585 (ns)
Phosphate	≥5 µm	1	0.122	0.019	1.062	0.449 (ns)
	0.22-5 µm	1	0.125	0.018	1.026	0.331 (ns)
Silicate	≥5 µm	1	0.043	0.007	0.372	0.987 (ns)
	0.22-5 µm	1	0.064	0.009	0.53	0.923 (ns)
Residual	≥5 µm	42	4.699	0.744		
	0.22-5 µm	42	4.986	0.714		
Total	≥5 µm	51	6.316	1		
	0.22-5 µm	51	6.988	1		

Table S 7: Variance inflation factors (VIF) for environmental predictor variables used in envfit and PERMANOVA analyses.

Environmental Variable	VIF
Chlorophyll *a*	3.05
Silicate	2.81
Temperature	1.57
Phosphate	1.57
Salinity	1.48
Nitrite	1.47
Nitrate	1.41
Ammonium	1.33

Acknowledgements

I am deeply grateful to everyone who supported me during this Master's thesis, each in their own special way. A particularly thank you goes to my two supervisors, Ingrid Sassenhagen for her expertise and guidance from start to finish, and Christiane Hassenrück for her outstanding bioinformatics supervision. Both were always available to provide advice and support throughout the entire process.

I would also like to thank the Bundesamt für Naturschutz (BfN, the German Federal Agency for Nature Conservation), especially Ronny Weigelt and the boat crew who made the sampling around the island of Vilm in the Greifswalder Bodden possible. I am very grateful for the use of their laboratory facilities on Vilm and for their flexibility in dealing with challenging weather conditions.

My thanks also go to Sarah Scholze for her active help during sampling, Philina Borowski for her support with all my questions, and Christian Meeske, Christian Burmeister, and Tuana Özkaya for their assistance in the laboratory.

Finally, a special thank you goes to my family and friends for their support during this thesis. Above all, I would like to thank Raphael Neiling for making this time so much easier for me.

Tools

This essay was translated, corrected and rephrased using ChatGPT (OpenAI, GPT-5.3, 2025, 2026), Gemini (Google, 3.1 Pro, 2026) and DeepL SE (Translator and Write). Literature research and organization was conducted using Zotero, ResearchRabbit, Google Scholar and NotebookLM (Google). Perplexity AI (Claude Sonnet 4.6, Anthropic) was additionally used for assistance in generating and identifying R code.

KI-Statement

Diese Arbeit wurde mithilfe von KI-unterstützten Modellen erstellt, zur Hilfe beim Übersetzen, Schreiben und Formulieren sowie Anpassen der R-Codes für die Datenauswertung.

Fragestellung, Datenauswertung, Interpretation sowie Einordnung der Ergebnisse in den wissenschaftlichen Kontext wurden vollständig eigenständig von mir erarbeitet.

Rostock, 30.03.2026

Supplementary Information

All environmental data, raw sequence data, and processed sequence files were uploaded to the internal server of the Leibniz Institute for Baltic Sea Research Warnemünde (IOW).

Environmental data: /bio/Raw_data/IOWseq000076_HABBAL2/Contextual_data

Raw sequencing data: /bio/Raw_data/IOWseq000076_HABBAL2/Seq_data

Primer-trimmed (clipped) sequence data:
/bio/Analysis_data/IOWseq000076_HABBAL2/Validated_data/GB18S_v1.

All analysis scripts used in this study are available at:
https://git.iow.de/bio_inf/IOWseq000076_HABBAL2/src/branch/main/R_scripts.

Eidesstattliche Versicherung

Ich versichere eidesstattlich durch eigenhändige Unterschrift, dass ich die Arbeit selbstständig und ohne Benutzung anderer als der angegebenen Hilfsmittel angefertigt habe. Alle Stellen, die wörtlich oder sinngemäß aus Veröffentlichungen entnommen sind, habe ich als solche kenntlich gemacht.

Die Arbeit ist noch nicht veröffentlicht und ist in gleicher oder ähnlicher Weise noch nicht als Studienleistung zur Anerkennung oder Bewertung vorgelegt worden. Ich weiß, dass bei Abgabe einer falschen Versicherung die Prüfung als nicht bestanden zu gelten hat.

Rostock,

30.03.2026

Ich bestätige, dass ich den Gutachtern fristgemäß eine elektronische Fassung meiner Abschlussarbeit zur Verfügung stelle.

Rostock,

30.03.2026
